Supersonic Nozzle Experiment

By Jeffery Fennell, Samantha Griggs, Miles Kim, and Caleb Nelson

Prepared for
The Edward F. Cross School of Engineering
Walla Walla University

Submitted in Partial Fulfillment of
The Requirements in
Capstone Engineering Project
May 24, 2022

I. Executive Summary

The purpose of this project was to design a system for the Fluid Mechanics Laboratory at Walla Walla University which can be used to run experiments involving compressible flow. This will teach students to gather and analyze data, while also providing them experience with compressible flow in particular. This was accomplished through the design and implementation of a high-pressure tank system that blows out through a converging-diverging nozzle. The primary tasks which needed to be completed for this system included:

- Assembly and installation of the system pressurizing the tank to 600 pounds-per-square-inch
- Design of an optical system that could visually record the density changes present in the shockwaves produced by the nozzle
- Accomplishment of pressure and temperature measurement in the tank and the nozzle
- Implementation of software to record pressure and temperature data in tandem with the optical instrumentation system
- Testing of the entire system to ensure proper functionality and synthesis between the different subsystems involved
- Creation of educational materials to aid instructors and students in understanding and executing experiments using this system

The design of a laboratory experiment must meet a variety of constraints to ensure safety, effectiveness, and longevity. Some of these are listed below:

- Adherence to ASME codes and standards for pressure vessels, pressure instrumentation, temperature instrumentation, data-acquisition systems, and a variety of other miscellaneous categories.
- Compliance with OSHA codes and standards about noise pollution due to the pressurization and blowdown noise produced by the system.
- Consideration of educational standards set by Walla Walla University, ABET, and NWCCU

Over the course of the project, most of the above were accomplished, and those that were not still saw significant developments. However, there are still some issues and future tasks that have not been addressed. The most significant of these are as follows:

- The booster pump used to pressurize the tank is not currently functional. Additional troubleshooting and possibly repairs will be necessary in the future.
- Full testing of the system at maximum pressure was not possible due to the aforementioned problems with the booster pump. These must be completed before the experiment can be used in an educational setting.

Over the course of this project, a system consisting of a high-pressure tank and a converging-diverging nozzle have been implemented and mostly prepared for use in the Fluid Mechanics Laboratory. This system will provide students at the Edward F. Cross School of Engineering with higher quality education in the area of compressible flow, and will give them additional tools to be successful in their careers. The implications and potential impacts of this service are nontrivial and far-reaching.

II. Contents

III. Table of Figures

IV. List of Tables

V. Introduction

In the Walla Walla University Fluids Mechanics laboratory, there are experiments designed to help students understand pipe flow, channel flow, and external flow. Until this year, however, there have been no experiments that demonstrate compressible flow, a major area of study within Fluid Mechanics. Dr. Doug Thomsen, a professor of mechanical engineering at Walla Walla University, has been working with students to fill this educational gap in the laboratory for the last three years. Recently, he has supported two groups of students in designing and implementing a high-pressure converging-diverging nozzle system for their senior projects. The first group of these students consisted of Parker Bailey and Jonathen Stacy (Bailey, Parker et. al. 2020). They designed and manufactured a converging-diverging nozzle that could theoretically achieve supersonic flow under an appropriately high-pressure gradient. The second group included Karl Zimmer, Samantha Griggs, and Miles Kim, two of which are continuing the project this year (Zimmer, Karl 2021). These students designed and assembled the basic components of the system and mounted the supersonic nozzle on a pressure tank rated to sustain the 600-psi needed to create an oblique shockwave. This year's group included Jeffrey Fennell, Samantha Griggs, Miles Kim, and Caleb Nelson. The goal for this year was to finish the experiment and prepare it to be used in the Fluid Mechanics laboratory the following school year.

Compressible flow is best understood in the presence of shockwaves. Frank White, an engineering professor at the University of Rhode Island, states that shockwaves are "nearly discontinuous property changes in a supersonic flow" (White, Frank M. 2016, 593). Supersonic nozzles create these property changes when air at a certain pressure is released through the nozzle. Shockwaves are formed when air is traveling faster than the speed of sound, because as it slows down to the speed of sound, the waves bunch together and form large, discontinuous shifts in the properties of interest. By measuring the pressure at different points in the nozzle as well as the pressure and temperature in the tank, students will be able to verify the compressible flow equations they learn about in class and in White's *Fluid Mechanics* textbook (White, Frank M. 2016, 593-681). Along with pressure exploration, Dr. Thomsen would like students to be able to see a visual representation of the shockwave's shape and how it corresponds to the numerical data provided by pressure measurements.

A. Project Description

This project had four main components, each of which provided ample opportunity for engineering problem solving. These divisions were: the assembly and installation, optical instrumentation, pressure and temperature instrumentation, and educational preparation. The pressure and temperature division of the project had two subsections: physical instrumentation and software development.

The assembly and installation section of the project was aimed at meeting a variety of goals that would allow the device to function safely and properly. It was important to consider installation codes, standards, constraints, and impacts, while also ensuring proper assembly of all parts relating to the device. Proper installation of the device within the Walla Walla University Fluid Mechanics laboratory was also necessary. Finally, steps were taken to execute finishing touches to the aesthetic attributes of the device per Dr. Thomsen's request. The supersonic nozzle device provides an environment for students to explore the nature and theory of compressible flow within the convenience and safety of the Fluid Mechanics laboratory.

A variety of specific tasks were required to effectively construct and implement to the supersonic nozzle device. These tasks included taking measurements of prospective spaces within the laboratory for installation as well as designing two-dimensional and three-dimensional models of a draft device to finalize layout plans. It was also necessary to analyze potential failure mechanisms, and ensure stakeholders approved of our preliminary proposal. Holes were drilled into the nozzle normal to the inner surface, and pressure instrumentation was attached in a way that allowed the pressure at that inner surface to be directly measured. When CAD models of the device were completed and approved, construction and installation of the device and its instrumentation were executed. Then, some final tests of the device and finishing touches were completed before regular use.

In order to build intuition about compressible flow, students need to be able to see the orientation of the shockwaves progress from oblique to normal. Because shockwaves are invisible to the naked eye, an imaging system that clearly shows the air density changes that come with shockwaves was required for this project. A common way this is accomplished is through schlieren imaging. In layman's terms, a schlieren imager provokes light passing through variable density air to refract in different directions. When some of these rays are blocked from the viewer, a shadow is cast where the light traveled through a specific density. Due to the range of densities encountered, a gray scale image appears of the air density in the region the light passed through.

Additionally, the students need pressure and temperature data from the experiment to understand compressible flow in the nozzle from a mathematical standpoint. The pressure and temperature instrumentation section of the project was aimed at accomplishing two tasks. First, a series of measurements of the pressure and temperature within the tank needed to be gathered, as well as the pressure at various locations along the nozzle. Second, results from the measurements had to be viewable both during and after the experiment, so they could be compared with compressible flow theory in converging-diverging nozzles. This data was to be as accurate as possible to demonstrate compressible flow from a data analysis standpoint. The two tasks just mentioned made up the two subsections of this division of the project. In order to accomplish the first task, holes were drilled into the nozzle normal to the inner surface, and pressure instrumentation was attached to allow the pressure at that inner surface to be directly measured. Then, an instrumentation package involving an electronics setup for collecting the data was assembled. To complete the second task, a custom computer software package for processing, storing, replaying, and visually representing the data was developed and tested.

Finally, a series of relevant documents needed to be prepared to facilitate a Fluids Laboratory experiment showcasing the project and assisting students in exploring the topic of supersonic flow. Following the format of current Fluid Mechanics Laboratory experiments, a laboratory handout, introduction video including instructions and safety information, and laboratory report key were needed in physical and digital format to provide Dr. Thomsen with a pre-defined set of objectives and goals for students to meet during their operation of the device. Though only a laboratory handout has been created at this time, once the experiment is fully functional, the other educational materials should be simple to make.

B. Literature Review

The study of converging-diverging nozzles, while quite simplified in undergraduate courses, is still something of great interest to researchers today, and models have still been developed within the last twenty years to understand them better (Chen, Shuxing 2009, 75-106).

Such nozzles can be very complex and are of immense practical value in a variety of fields. For example, in the area of plasma physics, converging-diverging nozzles have been used to control arcs in high-voltage anodes, allowing for better performance of the anode (Huang, He-Ji et. al. 2018, 847-852). These nozzles have also been used to launch medical treatments or drugs into human skin at supersonic speeds (Liu, Yi et. al. 2007, 1814-1821). The most common application of these nozzles, however, is in aerospace. Due to their ability to quickly accelerate fluid to supersonic speeds, converging-diverging nozzles are widely used as rocket nozzles, which have applications in spacecrafts, aircrafts, and missiles (Barbour, Ethan et. al. 2012) (Barbour, Ethan et. al. 2004) (Bose, T.K. 1967) (Jee, Craig et. al. 2020, 496-509).

While the construction and installation of the physical supersonic nozzle device and support table was not a mathematically intensive division of the project, there is still background information that was important to the success of the process. First, considering academic projects similar in scope and size of the construction and installation to our project, a variety of wooden tables were considered. One, reported on by Robert Keller, reports on the construction of a "one-hour" workbench whose design was the primary inspiration for the supersonic nozzle device stand (Keller, Robert J. 2019). Along with the initial design of the stand, a series of force calculations for determining the safety of the device from R.C. Hibbler's Mechanics of Materials, recommended by Dr. Qin Ma, a mechanical engineering professor at Walla Walla University, were used for considering the max shear loads, bending moments, and stress flows on members and fasteners of the stand (Hibbler, R.C. 2017, 293-300).

As for the optics section of the project, schlieren imaging has been largely used since the 19th century by astronomers and professionals in other fields that require "visualizing fluctuations in optical densities" (Davidhazy, Andrew 2006, 1-59) (Mazumdar, Amrita 2013, 1-16). Today, it is often used in fluid mechanics because it does not affect the flow of the fluid even as it is observed (Mazumdar, Amrita 2013, 1-16).

In Schlieren imaging, a point light source passes through a converging lens to create collimated light. The fluid of interest is placed in the path of the collimated light and another converging lens is placed farther down the system to focus this light. At the focal point, a knife edge is placed to cover half of the light source. The remaining light that is not cut off by the knife edge will pass and show on a screen or camera. The light that is cut by the knife edge creates a shadow. The basic system for a schlieren imager is shown in **Figure V-1**. This results

in a gray-scale image of density change. An example of this result, produced by our group's first iteration of a schlieren imager is also shown in **Figure V-1**.

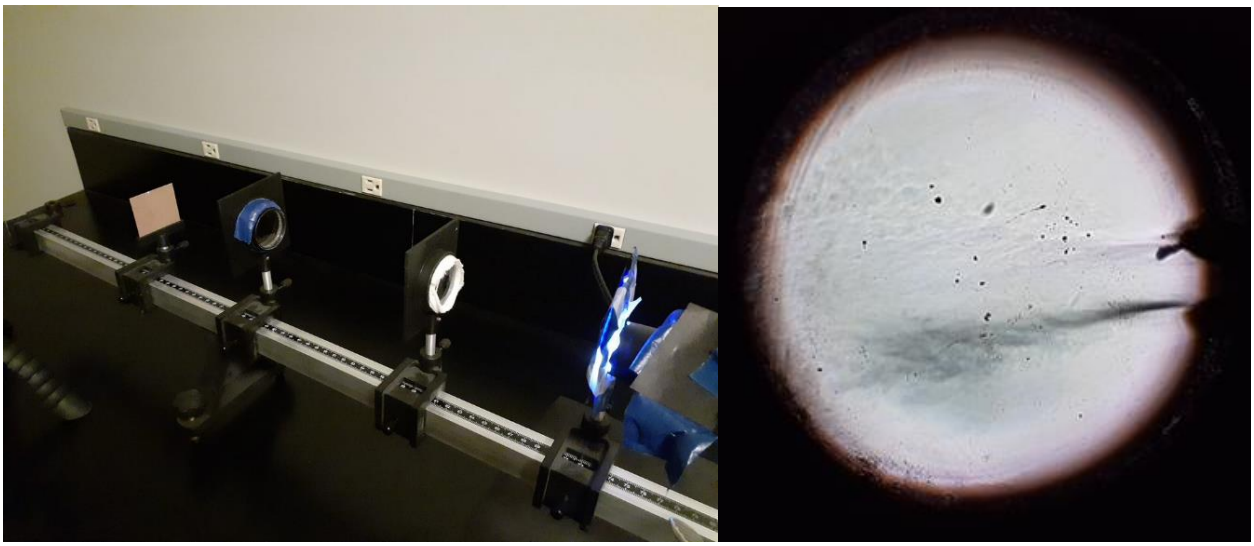

Figure V-1*: Schlieren imager setup and preliminary image*

Significant research into improving schlieren photography has taken place since the invention of the method in the 19th century. Because the concept of schlieren imaging is incredibly simple, schlieren imagers have been implemented in a wide variety of settings, including laboratories, garages, and even living rooms. One example discovered through one of these experiments, was replacing the knife edge with colored film so that different densities appear as different colors. Rainbow schlieren images can be used to show density gradients clearer than their gray-scale counterparts, but the actual image produced can sometimes be more confusing to the viewer. As a result, the imager designed for this project uses a knife edge to create the shadow (Mariani, R. et. al. 2019, 218-228).

VI. Problem Definition

This project was aimed at producing a fully functional converging-diverging nozzle system for the Fluid Mechanics laboratory, and had four different sections, each with its own goals and challenges. The four divisions were: assembly and installation, pressure and temperature instrumentation, optical instrumentation, and educational preparation. As mentioned previously, the pressure and temperature instrumentation division of the project was split into two subsections.

The first division of the project addressed the assembly and installation of the supersonic nozzle device and instrumentation. The general assembly of the device included a 30-gallon tank, a booster pump to pressurize the tank, pressure, temperature and optics instrumentation, and a device stand for the tank and supporting instrumentation. The support table served as a spot for the tank and instrumentation devices to attach to as well as a means of elevating the tank. By elevating the tank, built up fluids could be drained to prevent rusting. An outline for the assembly and installation of the device and instrumentation included the following: taking inventory of all items procured by previous groups' iterations of this project, designing floor plans and stand assemblies, analyzing force calculations on the preliminary designs, procuring parts for these designs, manufacturing specific parts, and installing the device.

Little progress was made on the assembly of the device stand and pressurized fittings by previous groups' iterations of this project. In 2020, Karl Zimmer began work on the layout of pressurized fitting assembly downstream of the pressurized tank. However, significant work was still required upstream of the tank and booster before the project was capable of standard operation within the Fluids Laboratory. To assist in picking up assembly and installation requirements from the previous groups, outside advisement was sought out from field experts such as Karl Zimmer, engineering professors, and Facility Support Services staff at Walla Walla University for the design, layout, and installation of the device.

To accomplish the specific tasks regarding the installation division of the project, key stakeholders in the project were contacted for consultation and assistance. For preliminary designs and parts lists, meetings were held regularly with Dr. Thomsen to seek advice on specific design constraints and applications. Through consultation with Dr. Thomsen, scope of the supporting table and deliverables such as weight requirements and optional shelving were developed to satisfy the needs of the Fluids Lab. To determine whether the initial designs for the device stand could satisfy loading requirements, force calculations were carried out in consultation with Dr. Ma to consider whether the stand would tip when loaded incorrectly, fail due to the applied load, or split at its seams due to shearing. Consultation meetings were held with the Facility Support Services of Walla Walla University to guide and assist in installation of certain pieces of the device such as the booster pump installation and plumbing upstream from the booster pump. Finally, for the manufacturing of the device stand, a parts list was created and ordered from Home Depot to create and assemble the device hand.

For the optical aspect of the project, the objective was to create a grayscale schlieren imager that shows the creation and withdrawal of the shockwave created by the supersonic nozzle. The imager could only capture the fluid within the collimated light between the lenses. Thus, the lenses used were large enough in diameter to encompass the nozzle's exit diameter with room to spare. A mounting system was designed and assembled so the image will not shake or become unfocused. This mounting system includes two converging lenses, a light source, an aperture to create a point light source, and a camera to capture the image. This system has been integrated with the pressure and temperature instrumentation so all three types of instrumentation measurements can be read simultaneously.

The pressure and temperature instrumentation division of the project specifically addressed the quantitative observation of compressible flow within the nozzle. This was accomplished through the measurement of static pressure at various points within the nozzle, and this data's comparison to the theory underlying converging-diverging nozzles. Compressible flow in converging-diverging nozzles follows a specific set of equations under the assumption of steady, one-dimensional, isentropic flow at every point in the nozzle except across any normal shockwaves present in the nozzle. Normal shockwaves have a similar set of equations associated with the property changes across them. These equations define the pressure, temperature, density, speed of sound, and Mach number at each location in the nozzle, and are driven by the pressure within the tank, called the stagnation pressure, at each point in time. Thus, the measurement of pressure at four different locations in the nozzle provides enough information to ascertain whether the compressible flow equations are consistent with the observed data. Pressure measurements within the tank itself were vital due to the appearance of tank pressure in the compressible flow equations. Additionally, the initial mass of air being discharged by the tank through the nozzle is reliant on density, which can be calculated from the pressure and temperature in the tank. Thus, temperature measurement within the tank was also necessary.

In previous years, other engineers have addressed this issue, but never actually implemented a solution to it. Jonathen Stacy, a previous student who worked on this project, created a model in SOLIDWORKS in which five separate holes were drilled normal to the internal surface of the nozzle at a variety of different locations along the nozzle in order to fully capture the behavior of pressures within the nozzle (Bailey, Parker et. al. 2020). However, no work had been done up until this year on actual pressure instrumentation, and the work previously done in SOLIDWORKS still had to be verified. Additionally, Karl Zimmer completed calculations related to the pressure in the tank over time based on the mass flow of the air exiting the tank through the nozzle, which was helpful in determining properties at various times along the nozzle.

This specific project had a clear set of tasks associated with it, most of which have been completed. The first task was the design and implementation of the physical instrumentation system. In preparation for this, calculations were completed to predict what pressures are expected at each point in the nozzle. A set of pressure sensors was then selected, considering the maximum and minimum pressure predicted at each location within the nozzle, to achieve the proper accuracy and to avoid the destruction of the sensors through loading outside of their operating regime. A thermocouple was also selected for the tank to measure its temperature. After this, a system by which the pressure at the surface of the nozzle was to be read by the pressure sensors was devised, and a plan to drill holes in the nozzle corresponding to this was required. These holes were drilled perpendicular to the face of the nozzle to avoid skewing the pressure readings by the addition of dynamic pressure from the supersonic flow.

Once the holes were drilled, the instrumentation was installed as planned so the pressure sensors directly measure the pressure at each important location. Before completion of this task, however, the instrumentation system by which the pressure sensor data is collected was implemented. This process involved obtaining amplifiers, an analog-to-digital converter, and a computer system to be set up to store and display the data on the computer.

The second task associated with the pressure and temperature instrumentation was the processing of this data. The data gathered using the physical instrumentation system needed to be processed and displayed in a visually appealing and easily comprehensible manner on the computer, which required software development. This involved reading data from the ADC, reading video information from the optical instrumentation camera, and writing software to synthesize, display, record, and replay this data in a visually understandable manner.

A laboratory report and instructional video also needed to be prepared before the project could be considered complete. To do this, the data to be collected from the experiment, as well as how that data is collected, was carefully considered, and a laboratory report handout was created. However, due to some setbacks, there are still some tasks that must be completed. A team must still attempt a first trial run of the experiment to collect measurements and create instructions, explaining how to successfully operate and collect data from the device. Once this has been successfully completed, the lab report handout should be updated with instructions explaining how to carry out this section of the laboratory. The lab report must then be presented to Dr. Doug Thomsen to ensure it meets his educational requirements. After his approval, a video must be made as well as a companion to the lab report with clearer, detailed instructions on how to conduct the experiment. Finally, using the laboratory handout and video, a team must attempt a second trial of the experiment and produce a laboratory report based on it, which will be revised until Dr. Thomsen approves of it. As a result, the laboratory report generated can be used by Dr. Thomsen in future years as a key.

VII. Objectives

A. Performance Requirements

This project had many performance requirements, considering the various divisions involved. The device stand and its instrumentation had several requirements for it to be approved for regular use in the Fluids Laboratory. Regarding construction, the table holding the pressurized tank and instrumentation was required to bear the minimum weight of the devices resting on it. A safety factor account for the weight of two students who might be tempted to sit, stand, or jump on the table was also considered. Next, the stand was required to be compatible with its instrumentation, allowing the instrumentation and pressurized components to be easily removed and reattached for servicing and operational checks. Third, the device stand was required to be large enough to hold all of its necessary components, but small enough to fit within the limited real estate of the Fluid Laboratory. Additionally, the stand would need to elevate the supersonic nozzle device to a height that would allow users to easily operate the device without needing to lower or raise their center of gravity to a level of discomfort, while still allowing the tank enough room below to drain excess fluids to prevent internal rusting.

The performance requirements for the optical instrumentation were highly variable. The main purpose of the instrumentation was to capture a visual representation of the shock wave to aid in students understanding of the physical phenomena. Due to the importance of these visual representations, the lenses could not be cloudy, the camera had to be able to focus on the shadow created by the air density, and the mount needed to not damage the image or blur due to vibrations.

The pressure measurement and data acquisition systems had a variety of requirements in order for it to function properly. For example, the holes that were drilled into the nozzle needed to be normal to the inner surface to prevent the supersonic flow from spilling into the pressure tap and adding its dynamic pressure to the static pressure that is to be measured. This could not be achieved with perfect accuracy, but it was important that the hole reached the surface as close to normal as possible. Similarly, it was important that each pressure tap reached the surface at the appropriate cross-sectional area. This, again, was difficult to ascertain with our tools and the shape of the nozzle. However, the physical construction did look nearly identical to the SOLIDWORKS model, which was ideal.

Additionally, the pressure sensors themselves needed to be able to measure the pressure ranges expected at each cross-sectional area. In order to accomplish this, the ranges were be theoretically predicted using the supersonic flow equations for converging-diverging nozzles found in White's *Fluid Mechanics* textbook (White, Frank M. 2016, 593-681). Then, the pressure sensors had to be able to handle the predicted pressures and measure to within ten percent accuracy at the lowest pressure within that range. This way, the data would be intelligible to students who engaged in the experiment. The pressure sensors also needed to have a response time that could measure the pressure changes at the rates at which they occur in the system.

As for the educational preparation section of the project, it was important that the laboratory handout, video, and sample key were easy to understand and intuitively describe the experiment in sufficient detail, while allowing students to still discover and learn from the experience.

B. Codes and Standards

There were a variety of codes and standards that needed to be adhered to for the success of the project. For the assembly and installation section of the project, adherence to several American Wood Construction (AWC) standards, university standards, and state guidelines directing the development and installation of the device stand and relevant parts was necessary. Because the construction of the device stand had to be accomplished primarily using hardwood lumber, the construction and safety of the table needed to align with the requirements outlined in the AWC M.3.1-2018 codes for general bending, tension, compression, and weight-bearing requirements (AWC EWC 2018). Along with the AWC structural requirements for the stand, ASME also outlined recommendations and requirements for construction with wood screws. These requirements were considered in accordance with ASME codes B.18.6.1 to ensure integrity at the joints of the device stand. Finally, to determine a set "home" location for the device and device stand within the Fluid Mechanics Laboratory, University recommendations (McVay, John 2020) as well as Washington State guidelines (Washington State Legislature) were considered for the safety of Fluid Mechanics laboratory students, teachers, and technicians who might be operating and/or servicing the device in the future.

Safety measurements such as those pertaining to noise exposure and pressure vessel standards were also considered to minimize risk of injury during device operation. The Occupational Safety and Health Administration (OSHA) requires that protection against the effects of noise exposure be provided when sound levels exceed 97 dBA for 3 hours (OSHA OSHS 1910.95). Because the supersonic nozzle will expose all users to noise volumes above this limit, the lab handout requires that students use noise protection provided by the lab assistant during device operation. The ASME Boiler and Pressure Vessel Code (ASME BPVC.VIII.1) outlines regulations for creation of pressure vessels safe for operation. The 30-gallon tank purchased from McMaster-Carr notes that the pressure vessel both meets this standard as well as another ASME code that requires the tank to be water tested and rusted on the interior of the tank.

There are many standards for designing and manufacturing optical equipment that are used in high stakes applications. However, because this project did not use lasers or any other optical equipment that will pose a threat to students, adherence to strict optical codes and standards relied more heavily on the construction tolerances rather than safety measures.

On the other hand, compliance to several ASME standards was also required for the pressure and temperature instrumentation portion of the project. Since the project involved pressure measurement and instrumentation, it was important to take the ASME PTC 19.2-2010 codes for pressure measurement into account when designing the system (ASME PTC 2010). Additionally, since temperature was to be measured in the tank, the temperature measurement system had to be in alignment with the ASME PTC 19.2-2010 code (ASME PTC 1974). The ASME PTC 19.2-2010 codes for data acquisition systems were also important in the design of the analog-to-digital converter interface with both the computer and the transducers being used to measure pressure and temperature (ASME PTC 2008).

There are also several educational codes and standards that had to be met or at least considered in the completion of the laboratory materials. First, there are standards set by the Walla Walla University School of Engineering that had to be strictly followed in this process. These include the laboratory report standards, graphing standards, and Fluid Mechanics Laboratory syllabus provided by the university (EF Cross School of Engineering 2017) (Thomsen, Doug 2021) (Yaw, Louie et. al. 2016). Additionally, other organizations that provide

accreditation to the engineering program at Walla Walla University, such as the Accreditation Board for Engineering and Technology (ABET) and the Northwest Commission on Colleges and Universities (NWCCU), have requirements that needed to be considered.

C. Constraints and Impacts

Along with the codes and standards for this project, there were constraints under which our project must abide. The project also had several short-term and long-term impacts. The study of this supersonic nozzle system by Fluid Mechanics students in the future will be of great benefit to their education and understanding of compressible flow. It will allow them to build some intuition on the topic, allowing them to carry a stronger understanding of these topics into their careers and prepare them for effective engineering practices after college.

The portion of the project involving construction and installation of the device stand and its instrumentation has several impacts on the environment and future of the Fluids Laboratory. The size of the project occupies a significant portion of the laboratory, meaning that devices that had been deemed "out of commission" needed to be removed or repurposed to make space for the new project. The primary impact of the device considered was the effect of the booster pump on the surrounding environment of Kretschmar Hall. Because the booster pump required compressed air to both drive and compress air through the pump, there was concern that the pump would "suck the shop air dry" throughout the basement of Kretschmar Hall during usage. The amount of noise produced while pressurizing the tank, and later while running the experiment, was also an environmental concern. If the experiment was too loud, the sound could travel down the halls of Kretschmar Hall, disrupting classes and causing general noise pollution within the building. The booster pump already had a muffler included with it to reduce the noise, partially ameliorating this issue. Additionally, when testing the experiment, the noise level outside of the lab was also examined to see if additional measures were necessary. After consideration, no such measures were deemed as necessary.

The supersonic nozzle project also had a couple constraints that must be met in the completion of its design. First, Walla Walla University and the Fluid Mechanics Laboratory in particular had limited funds which could not be freely spent without thought. One of the primary aims of this project was to create a system to study compressible flow that was significantly cheaper than alternative options available on the market. This meant that each time a part was ordered, especially if it was expensive, it was important to research the most cost-effective option for the needs of the project. Additionally, if an expensive purchase was needed for a particular function in the project, that aspect of the project was examined to see if it is absolutely necessary, or worth the financial investment.

The project was also required to provide a safe learning environment for future students. This meant that, as it was being assembled, significant care was required to be put into ensuring the experiment would not cause damage to its surroundings. This included ensuring proper installation of all fittings and tubing that was installed. Additionally, the pump used to pressurize the tank, as well as the device itself, had the potential to be very loud. Based on the decibel level of the device, it was decided that ear protection should be used during device operation in the laboratory for the duration of the experiment. This is not a significant issue, however, because ear protection is generally necessary in the lab for the other experiments that will be running concurrent with this one. The instrumentation system needed to be easy to use and access by the students as well. This included having an easily accessible interface with which to interact and collect data.

The primary set of constraints for the imaging division of the project dealt with physical parameters. Finding lenses, cameras, and light sources that are inexpensive was not difficult. However, making sure that the optical system did not shake while the experiment was running, as well as ensuring the light source did not overheat, is not as simple. As the project proceeded, these constraints were considered during the synthesis of this instrumentation. Students will now be able to visualize the shockwave produced in the nozzle as well as any other future density change projects in the lab with the schlieren imager.

The laboratory report, video, and sample key have the potential to be the most impactful part of this project. By providing students and Dr. Thomsen with clear instructions and guidance on how to conduct the experiment, and by allowing students to explore compressible flow in a hands-on environment with clarity, this project has the potential to have a significant societal impact. It will do this by increasing the quality of education provided by the Fluid Mechanics Laboratory in the years to come. For example, students will gain analysis experience through studying data gathered during the experiment. The practice students will gain from this data analysis will increase their proficiency as engineers. As a result, they will be more likely to effectively and intentionally gain an understanding of physical phenomena based on collected data in the course of their professional work. To ensure such an outcome, the laboratory handout was made to be short enough for students to be able to complete it within a reasonable time frame, but long enough to provide a stimulating challenge. Finally, each page of the report was fit within a normal printed page.

Although the project will have long-term, indirect societal impacts, there is no sure way to measure the impact of the project on a global scale. It is possible that the improvement of the engineering program will produce more capable engineers, and that these engineers will eventually work on projects with global implications. However, it is unlikely that such an outcome will be significantly impacted by this experiment. Thus, there are no anticipated global impacts associated with this project.

VIII. Assembly and Installation

The general assembly of the supersonic nozzle device includes a 30-gallon tank, a booster pump to pressurize the tank, instrumentation (pressure, temperature, optics), a device stand for the tank and supporting pressure and temperature instrumentation, and an optics stand to support the optics instrumentation. While the conceptualization and mathematical verification of this device has spanned across several years, practically no progress had been made on the installation of the device until this fall. With a goal of completing the project by Spring 2022, it was important to create a rigorous list of installation tasks that would need to be completed to ensure the device would be working by the end of the academic year. This list included installing the booster pump, plumbing and filtering to supply the tank and booster pump with shop air, procurement and installation of high-pressure fittings, and procurement of parts for and installation of device and optics stands.

A. Device Location Selection

Following the project proposal presentations in early Fall 2021, the transition from hypothesizing the design of the supersonic device to actual construction was quickly made to ensure necessary tasks could be accomplished within a reasonable timeline. To begin assembly and installation of the device, a location for the device was the first consideration. Several locations within the Fluid Mechanics Laboratory were considered, however, an opening at the

northwest corner of the laboratory was selected. This location is depicted clearly in **Figure VIII-1.** To provide for a safe learning environment, this location was selected for the lower amount of foot traffic that would take place on the west end of the lab during simultaneous operation of other devices in the lab during normal instruction periods. This location also provided for enough room for pressurized air exiting the nozzle to diminish drastically in speed before coming in contact with any surrounding equipment or walls – greatly reducing risk of damage or erosion to the surrounding environment. Finally, this location adhered to safety codes and standards considered during installation – mainly International Fire Code Standard 605.3, stating, "A working space of not less than 30 inches in width, 36 inches in depth and 78 inches in height shall be provided in front of electrical service equipment." For this reason, a device location along the west end of the lab was not selected, so as to not obstruct the electrical breaker boxes occupying a majority of the wall.

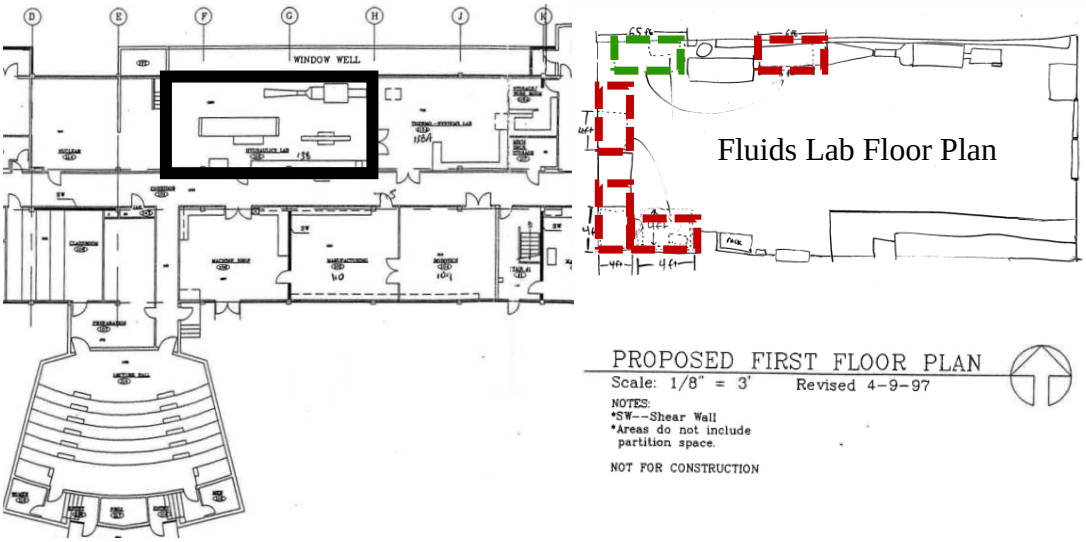

***Figure VIII-1**: Device Stand Location Selection. Right: Fluids Laboratory of Walla Walla University. Left: Alternative Locations Considered*

With a location selected for the device, finalizations were made to the location of the device such as distance from either of the walls which the device would be placed against, size of the device stand, and location of the booster pump and filter. Factors considered during these finalizations included potential future repairment procedures, ease of operation, and obstruction of windows. To provide a visual aid in this process, painter's tape was used to present a projection of the device onto the north wall of the Fluids Laboratory for approval by Dr. Thomsen. After approval was given, installation could begin.

B. Booster Pump and Plumbing Installation

The next logical step in the assembly of the device was to begin the installation of plumbing that would be required to pressurize the 30-gallon tank. To pressurize the 30-gallon tank, two pressurized lines are provided to the tank, one being supplied by the 120psi shop air line of Kretschmar Hall, and one supplied by the SC Hydraulic Engineering ABD-M204-5 booster pump. The shop air acts as a method to quickly ramp the 30-gallon tank's internal pressure up to 120psi, while the booster pump acts as the true powerhouse, supplying the extra boost of 600psi air required to run the supersonic nozzle at desired ratings. Rather than using an electrical booster compressor, a mechanical pump was selected by Karl Zimmer as a more cost-

effective alternative. The caveat to this mechanical pump is that it requires two 120psi supply lines to operate. Therefore, a total of three 120psi supply lines would need to be split across three inlets for this supersonic nozzle device in total. There was concern that this design would deplete Kretschmar Hall of its pressurized air during operation of the supersonic nozzle device, but after consultation with the Walla Walla University campus plumber, Ron Wentland, it was decided that this issue was unlikely to arise during operation.

To guide in the installation of the booster pump as well as an upstream filter to rid the plumbing of any debris, Karl Thompson of Walla Walla University's Technical Support Services was consulted. Under the supervision and support of Karl, installation of the pump and filter was safely completed. After the installation of the booster pump, plumbing upstream of the pump could take place. An initial plumbing schematic was created under the guidance of Ron Wentland, the WWU campus plumber. Safety equipment including valves for each individual plumbing line, check valves, and an emergency shut off were considered in the proposal. The initial plumbing diagram is provided in **Appendix** A – Device Stand Assembly and Construction Visual Aids**.** With the proposal approved by Dr. Thomsen, installation of the upstream plumbing was completed with the help of Ron Wentland. The installed booster pump and upstream plumbing are depicted in **Figure VIII-2**.

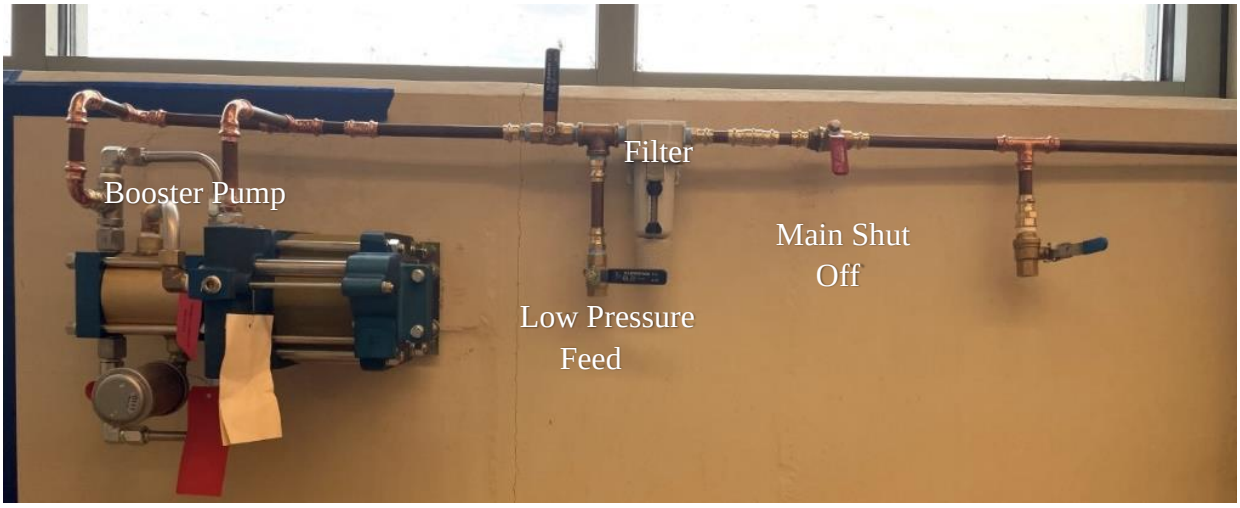

Figure VIII-2*: Installation of Booster Pump, Filter, and Upstream Plumbing*

C. Device Stand Design

Following the installation of all equipment upstream of the 30-gallon tank, a connection between the plumbing and tank had to be made to start testing the system. The device stand would serve as a load-bearing table, primarily bearing the weight of the tank, but also supporting any students or teachers who might be tempted to stand or sit on the stand. It would also elevate the tank, giving students a better view of the nozzle while allowing condensation to be periodically drained from the tank. Through consultation with Dr. Thomsen, the scope of the supporting stand and specifications such as weight requirements and optional shelving were developed to satisfy the needs of the Fluids Laboratory. To determine whether the initial designs for the device stand would satisfy the loading requirements, hand calculations were carried out to determine if the stand would fail in compression or buckling. To further analyze and verify the structural integrity of the stand, a finite element model was developed and analyzed. This provided more accurate information regarding the stress and deformation of the structure.

D. Hand Calculations for Device Stand

The hand calculations were solved for using material property information from The *Wood Handbook: Wood as an Engineering Material* (Forest Products Laboratory 2010, 5-3). Along with material properties, R. C. Hibbeler's *Mechanics of Materials* was used for reference with several stress, moment, and buckling calculations, which proved useful during the hand calculation analysis portion of this project (Hibbeler, R.C. 2017, 293-300).

The first hand-calculation performed for this project helped determine whether the plywood sheathing would fail in the normal direction under the weight of the tank that would be resting on top of it. Material properties were taken from Hibbeler's reference tables and used to simultaneously simplify the hand calculation and create a "worst-case scenario" for the table, the middle leg of the table was removed from the table. A shear moment diagram was created to verify that the assumption that the moment applied to the sheathing would occur at the center of the tabletop. By analyzing the moment at the center of the tabletop and using this maximum moment to solve for the maximum stress acting on the sheathing at the center of the tabletop, a load that provided a factor of safety of nearly 2 (for this worst-case scenario) was determined. These material properties and calculations are provided in **Figure VIII-3**.

$$\sigma_{wood} = 4890\frac{lb}{in^2} \qquad \tau = 885\ lb/in^2 \qquad E_{wood} = 1.01 \cdot 10^6\frac{lb}{in^2}$$

$$M_{max} = \frac{67.5"}{2}(125lb) = 4218.75\frac{lb}{in} \qquad \sigma_{max} = M_{max} * \frac{c}{I} = 2736.49\ psi$$

***Figure VIII-3**: Assumed Material Properties and Simplified Calculations for Determining Plywood Failure Design Factor*

The second hand-calculation considered for the analysis of the tank was used to determine whether or not the normal stress applied to the table legs by the weight of the tank would be enough to cause failure within the leg. Assuming that only a maximum of fifty percent of the tank's weight would be applied to any one of the legs at any given moment, an estimate "worst case scenario" was made using half of the tank's weight, acting on a single leg, to calculate an approximation of the normal allowable stress on the table legs. The equation for this normal stress analysis was taken from chapter one of Hibbeler's *Mechanics of Materials*. Solving for the distributed load, roughly 24 psi was calculated to be expected at the cross-sectional area

of the table leg. Because this stress is below the yield stress, it was determined that the leg would not fail. The material properties and calculations for this scenario are provided in **Figure VIII-4**.

$$\sigma_{fir} = 7230\frac{lb}{in^2} \quad E_{fir} = 1.95 \cdot 10^6 \frac{lb}{in^2} \quad \sigma = \frac{N}{A}$$

$$N = 50\%\ of\ 250lbf = 0.50 * 250 = 125lbf$$

$$A = 1.5 \text{ x } 3.5 = 5.25in^2 \quad \sigma = \frac{125lbf}{5.25in^2} = 23.81psi$$

***Figure VIII-4**: Assumed Material Properties and Simplified Calculations for Determining Table Leg Failure*

Another hand calculation that was used to compare against computer aided models was the first mode buckling of a table leg under the weighted compression of the tank. To determine whether the table legs would buckle under compression of the tank, an analysis of the leg using a column-buckling method with an effective length factor for a (worst case) fixed-fixed instance was conducted using the equations (taken from Hibbeler's Materials of Mechanics). The critical force was found to be much higher than any force that would possibly be applied to the legs of the table. Thus, it was determined that the device stand would not fail due to buckling. The material properties and calculations for this scenario are provided in **Figure VIII-5**.

$$P_{cr} = \frac{\pi^2 EI_x}{(KL)_x^2} \qquad \sigma_{cr} = \frac{P_{cr}}{A}$$

$$P_{cr} = \frac{\pi^2(1.95 * 10^6)(5.359)}{0.5\left(\frac{39}{2} * 12\right)^2} = 7534.36lbf$$

$$\sigma_{cr} = \frac{7534.36}{5.25in^2} = 1435.12psi$$

***Figure VIII-5**: Assumed Material Properties and Simplified Calculations for Determining Table Leg Failure*

E. FE Modeling for Device Stand

Quite a few of the assumptions made were necessary to attempt the finite element analysis in the first place. The first of these was the method used to construct the stand. The table was assumed to be constructed perfectly, so that all pieces were the proper shape without any consideration of manufacturing tolerances. Thus, all contacts were modeled as "bonded" in Ansys. For the scope of the failure analysis completed as part of this project, it was assumed that the wood would fail before the steel fasteners and glue. It was also assumed the supports at the feet of the table were fixed supports. Even though they would be able to slide a small amount on the floor of the Fluids Lab, it was decided that the table's displacement would be minimal. This assumption was necessary to solve the model in Ansys. Finally, the load was assumed to function as a remote load in Ansys, where the 250-pound load was evenly distributed among the four feet of the tank. Students standing on the table were also considered to be remote loads

distributed evenly over the area of their feet, which were modeled as rectangles with circular caps on the ends.

Several assumptions were made regarding material properties. First, the plywood top was considered to be isotropic, even though plywood has different properties in different directions. This was because no properties could be found about plywood to allow the model to be built as an orthotropic or anisotropic model. Additionally, the coastal Douglas fir members composing the frame were considered to be orthotropic, having different properties along three mutually perpendicular axes. Although the *Wood Handbook: Wood as an Engineering Material* listed nine independent major and minor Poisson's ratios, only the major Poisson's ratios were used so that an orthotropic material model could be utilized in Ansys. After calculating the minor Poisson's ratios from the major Poisson's ratios using basic relations developed in advanced materials textbooks, it was found that the error in this approximation was minimal.

In order to conduct analysis on the table using finite element methods, SOLIDWORKS was used to model the geometry of the table and Ansys to conduct the finite element analysis. Once the model was created in SOLIDWORKS, it was exported as a .step file and imported into Ansys Design Modeler. The plywood part was used to create a surface body that could then be defined using 3D shell elements in Ansys Mechanical. This was a critical simplification in the analysis to avoid errors encountered by trying to mesh such a thin component using 3D solid elements, while still allowing it to exhibit three-dimensional behavior in direct interaction with the wooden members. After the surface was created, the extra bodies representing the feet of the tank and student were imprinted onto the surface so corresponding forces could be applied over these areas.

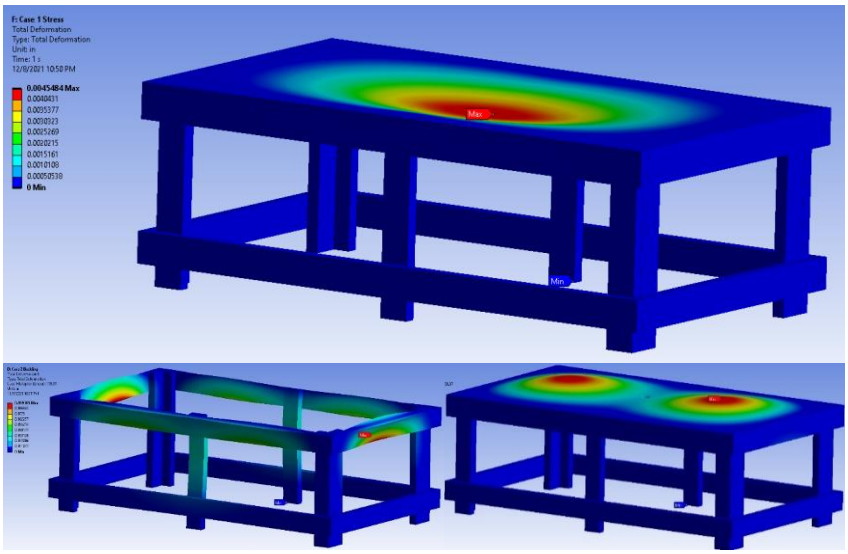

***Figure VIII-6**: Finite Element Analysis on Device Stand*

Overall, the hand calculations and determined stresses from the Ansys models agreed with each other. As expected, the Ansys stress calculations revealed a lower maximum stress in the tabletop due to the "worst case scenario" approach than those taken with the hand calculations. While the stress results from the hand calculations and Ansys were similar in magnitude, the expected maximum allowable buckling loads were not. For the Ansys calculations, an estimated maximum load of 40 tons would be required to buckle the frame, whereas a load of 7500 pounds would be needed to buckle the frame according to the hand calculations. This large variation in expected maximum loads was likely because the buckling hand calculation was taken along a single element of the frame, whereas the Ansys modeling

calculated the maximum load necessary to buckle the entire system – where single members were able to support or brace each other and work together against the load attempting to buckle the members. Because of this, the hand calculations provided for the buckling forces were much lower. Several images of this Ansys model are provided in **Figure VIII-6**.

The results of this loading scenario confirmed the table's structural integrity. The maximum von-Mises (equivalent) stress occurred at the top corners of the central members of the table, where the plywood that was deforming in a concave manner was pressing against the sharp corners at the top of each member. Thus, these points had significantly more stress than the rest of the members. It is important to recognize that these are stress concentrations, and the corners will not be perfectly sharp when the table is constructed.

Even with these areas of increased stress due to the limitations of the model, the corrected factors of safety for ductile failure (that account for the orthotropic properties of wood) for cases one and two were 5.24 and 3.57, respectively. Thus, the table will be able to support unexpected loads, such as students or supplies, in addition to the load of the tank while maintaining an acceptable factor of safety. The factors of safety provided by the stress tool were corrected to obtain these values as it was not possible to use the stress tool alongside the convergence studies due to lack of computer memory. The lowest factor of safety occurred at the same location as the maximum stress on each model.

Failure by buckling was also analyzed for each model. Mode one buckling occurred most severely in the central members of the table, but the critical buckling load was still 334.13 times greater than the applied load. This would be equivalent to a load of over 41 tons. Thus, failure will not occur by buckling. Mode two buckling was also analyzed and had a critical buckling load that was 364.56 times greater than the applied load. Buckling of the top was also analyzed, but due to the complex nature of composite materials such as plywood, it is likely that an isotropic model does not reflect the actual behavior of the top. These results are included for reference. However, the deflection shown as the top buckles matched intuition, assuming that all edges of the top were perfectly bonded to the frame.

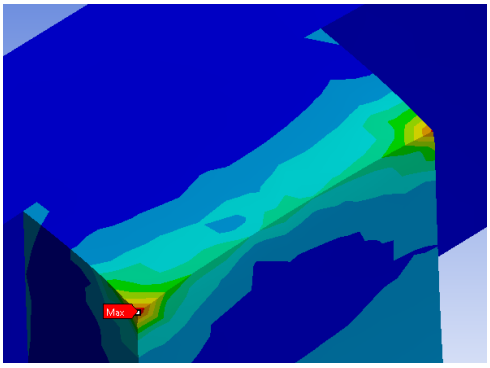

***Figure VIII-7**: High Stress Areas at Corner of Table Leg*

The last analysis for the table involved examining the stresses at each joint. The contact tool was used for this analysis. The maximum contact stress for this case in the normal direction to the joint surface was 1285.06 psi and the maximum shear stress was 765.18 psi. For a chosen fastener that meets these stress requirements, further analysis could be done to determine the required number of fasteners required at critical locations where the maximum stress at the contacts occurs. From the results, it was clear that extra fasteners will be required along the outer edge of the plywood where it is attached to the frame. The results also suggested that extra fasteners will also be required along the outer edge of the plywood where it is attached to the

frame as well as where the vertical members at each corner attach to the horizontal supports. The suggestions from this modeling were implemented during the construction of the table. A graphical representation of this high stress area is depicted in **Figure VIII-7**.

By comparing the factors of safety for ductile failure to the load multipliers from the buckling, it is clear that the failure mode will be ductile failure by exceeding the maximum von-Mises stress. However, the table will maintain its structural integrity as the lowest factor of safety is still 3.57 when considering the load of two students standing on the table in addition to the tank. Fatigue failure was not considered because the table will not be loaded and unloaded over a large number of cycles. Based on these results, there will be a significant safety margin to account for additional unexpected loadings as well as assumptions made during the analysis concerning the construction of the table, including the materials used. It will also help to account for any possible manufacturing defects.

F. Device Stand Assembly and Construction

When FEA was accomplished and approved by Dr. Thomsen, it was time to begin construction on the device stand. By creating a parts list ahead of time, material and money were saved during the purchase of equipment such as lumber and fasteners. The design plan for the device stand was followed almost exactly, with one exception. During the construction of the stand, the conceptualization of shelving under the table was considered, and the bottom brace of the stand was lowered to be flush with the ground as a design decision to allow for shelving to be installed after the construction of the device. After the stand was complete, it was polished, primed, and painted for aesthetic purposes, and the 30-gallon tank was placed on top of it to begin plumbing downstream of the booster pump. It should be noted that the device stand securely held the weight of the 30-gallon tank and two students with ease – accomplishing the goals set out by the stand. The unpainted stand with the tank resting atop it is provided in **Figure VIII-8**.

***Figure VIII-8**: Finished Construction of Device Stand with Tank, Unpainted*

G. Downstream Plumbing

Many of the parts needed to complete plumbing downstream of the booster pump had already been ordered before the stand was complete. Upon installation, the concern of thermal

expansion halted assembly and forced a reconsideration to the downstream plumbing plan. Originally, a "straight-shot" from the booster pump to the tank was intended for the design, however concern that the plumbing might expand during device operation and burst if no "give" were allowed to the pipes arose. Because of this, a thermal expansion "S" route was devised and parts necessary to complete this plan of action were purchased. This "S" would allow for give during expansion and compression of the high-pressure plumbing feeding into the 30-gallon tank. This revised plan involved using a high-pressure expansion hose which was believed to be rated for the pressure and temperature necessary for the purposes of this experiment. To verify the hose would not burst during operation, an Isentropic Relation taken from White's *Fluid Mechanics* was used. The calculations approved of the hose. It should be noted that the downstream plumbing also incorporated a secondary drain to mitigate any fluid buildup that may have slipped through the upstream filter. This created a subsequent line of defense against possible fluid buildup and rusting in the 30-gallon tank. Following verification by both Ron Wentland and Dr. Thomsen, installation was completed after necessary parts arrived.

H. Recent Work

At about halfway through the academic calendar, the conception of an optics stand was introduced to the scope of the Assembly and Installation division of the project to allow for the optics instrumentation to properly read data at the end of the nozzle. To ensure this second stand was built with enough time to complete the other divisions of the project, the plans and hand calculations for the original device stand were foregone by scaling the same plans for the device stand down. Although a scaled version of the original stand would prove to be well overbuilt for the uses of the optics stand, the use of the same design allowed for immediate progress to be made in the construction of the optics stand.

With both the device stand and optics stand constructed and installed, the beautification of this furniture could commence. Two to three coats of primer and paint were used to enhance to the visual appeal of the stands in the fluid mechanics laboratory as well as protect them from rotting, decay, and wear and tear that might occur with annual use. After the beautification of the stands was completed, they were connected using galvanized strong-tie braces and rearranged in the fluid's laboratory into their final resting spots.

Because plumbing and construction were being completed simultaneously, finishing touches on the installation and construction of the entire device were able to be placed as soon as the nozzle and device stands were finished and placed in their corner of the laboratory. Only a handful of tasks remained to consider the construction and installation division of the project as complete, all dealing with different aspects of plumbing. First, a pressure relief valve was installed to the backside of the 30-gallon tank to allow for the tank to release in the case of emergency. Although the lab handout that will be provided to students will stress the importance of not over-pressurizing the tank past 600 psi, the booster pump upstream of the tank has the potential to pressurize the tank up to 855 psi, ultimately introducing a high risk for injury if the tank were left unattended or unnoticed during pressurization. For this reason, a pressure relief valve has been installed to and will be calibrated to release pressure from the tank if it ever reaches an internal gauge pressure of over 590psi. Once pressure drops below the desired setting, the relief valve will lock once again and the laboratory will be able to be continued in a normal fashion. A locking mechanism will also be installed to the relief valve to ensure the calibration is not changed or modified by unaware students or technicians. The pressure relief valve and second feed are provided in **Figure VIII-9.**

Figure VIII-9: *Alternate View of Device Depicting Pressure Relief Valve and Tank Infeeds*

A drain to the underside of the tank was installed next to allow for drainage of potential fluid buildup. Although the McMaster-Carr 30-gallon tank has been water tested and internally rusted according to ASME standards, we would prefer for no further rust build up to occur during normal operation of the device. For this reason, a drain on the undercarriage of the tank has been installed. Students will be instructed to release any moisture or remaining pressure to atmosphere to mitigate potential damage to the tank and/or nozzle over time. Finally, a second tank inlet feed was installed to the upstream plumbing of the tank. This second feed, which utilized 120psi shop air, allowed for the tank to be filled first up to lower pressure levels, and only after this process was complete, would the booster pump be used as a second-stage device to do the rest of the "heavy lifting". By utilizing a two-process, the booster pump would ultimately be saved of some wear and tear from needing to pressurize the tank over the entire course of its filling time. The reason for the delay in installation of this second feed was because of shipping times in parts that were still needed for the plumbing of this line. As soon as the parts had arrived, the second line was installed, and plumbing was completed.

Now, with construction, installation, beatification, plumbing, and risk prevention completed, hardware tested could commence. During week two and three of the final quarter of project completion, the device was run for the first time at its full capacity. Upon running the device, an issue with the booster pump was identified and hardware testing halted. To our misfortune, the booster pump purchased from SC Hydraulic was unable to pressurize the tank to the desired pressure as it indicated it would be able to. Several possible reasons for this issue were explored, including cycling valve repairs, infeed plumbing, and flow rate calculations, all of which checked out, leaving us to believe that the issue must have been with the pump itself. Work is being conducted to return the pump to the manufacturer for repair. The entire finished assembly and installation of the device is provided in **Figure VIII-10.**

Figure VIII-10: *Finished Assembly and Installation of Device*

IX. Optical Instrumentation

As previously established, there are several ways to show the density changes in air. One method is to create a shadow graph. This is similar to a schlieren imager in that it has a point light source followed by lenses that create collimated light, while the fluid being studied is located in-between them. The light is projected onto a screen or camera after exiting the second lens. However, what differentiates a schlieren imaging system from a shadow graph is that the shadowgraph does not cut the light in half with a thin edge such as a knife edge. This simple addition takes the image formed by a shadowgraph and gives the pictures more definition.

To create a schlieren imager, four components are necessary before final mounting: a light, lenses, a camera, and a knife edge, as shown in **Figure IX-1**. We will look at each component and its mount design individually. The assembly placed at the end of the system houses both the camera and the knife edge. To get a good image, the camera needs to be very close to the light coming from the knife edge, so they were mounted in the same housing. The camera must be able to take video fast enough to capture the shock wave at mildly precise times to correlate with the data gathered from the pressure and temperature instrumentation. Most of

the details relating to the camera will be handled by the software development division of this project.

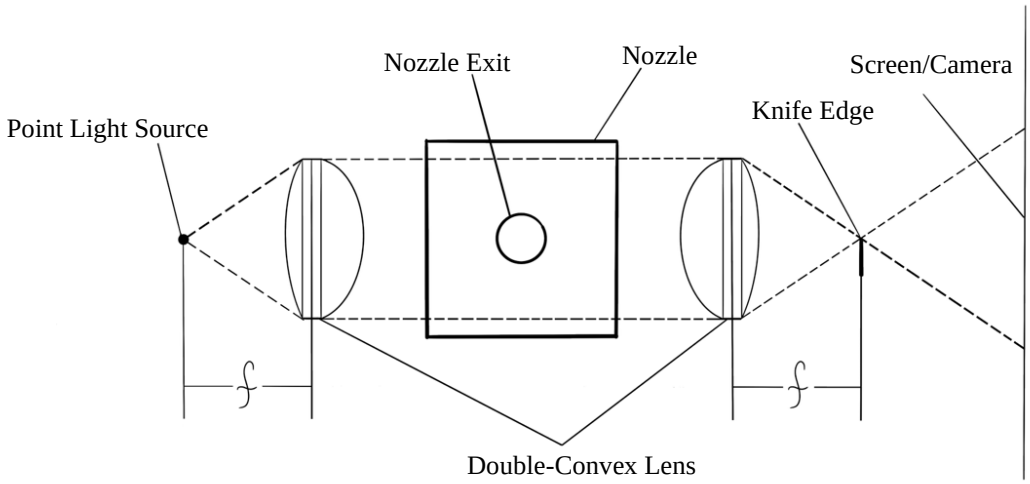

***Figure IX-1**: Schlieren Imager*

A. Lighting

The light is a very key element of the schlieren imager. It must be bright enough so the viewer can see adequate contrast between higher and lower density areas. Using a point source also keeps the final image clear and readable. Finally, diffusing the light will give an even intensity across the viewing area so parts of the fluid show up brighter or darker than they should. These parameters were taken care of through picking a light and designing the housing.

Light color, shape, and how ideal the point source is all impact the quality of the image coming out. We also need to be aware of overheating due to long periods of operation. We must also consider that the Fluid Mechanics Laboratory is a well-lit area. Both LED lights and lasers are bright enough to show the density change in air, but we chose to use a single LED over a laser for several reasons. As mentioned in previous sections, rainbow schlieren imaging can be used to analyze the density gradient in a flow field (Mariani, R. et. al. 2019, 218-228). However, for simplicity we decided to use a white LED and keep the gradient in gray scale. LEDs are also a good choice because they are cheap and very bright. Using a laser would add a color element to the image and may be harder to adjust for those making adjustments in the future. Many of the lights we used in testing came with quirks that affected the outcome of the picture because the light was not spread evenly. As a temporary fix, we used a piece of frosted glass to defuse the light. A piece of paper with a pin hole in it served as an aperture, creating a point source. The diffused aperture is shown in **Figure IX-2**.

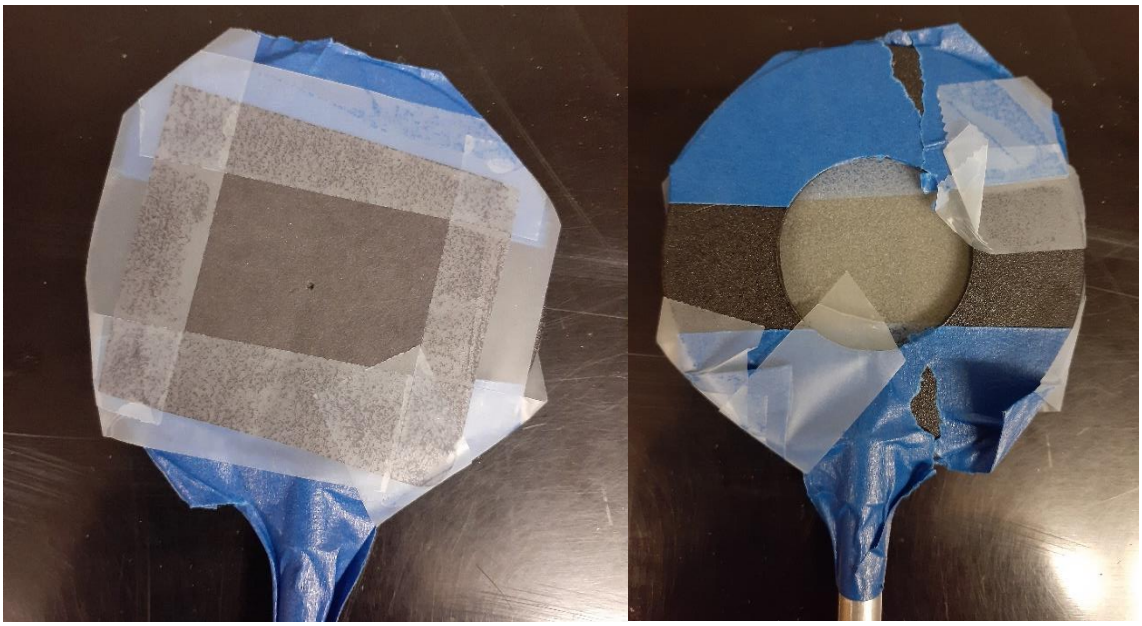

***Figure IX-2**: Temporary Aperture and Diffused Glass*

The final design of the light source is still in progress. However, we want to diffuse the light and incorporate the aperture into the housing that holds the white LED. The mount for the light will be similar to that of the lens mount shown later in this section. It will most likely be a box with a slit to add or remove the diffuser. There will be a small hole in the front to act as an aperture.

B. Lens Selection, Placement, and Housing

The lenses are what focus the light. They need to be clear of blemishes and held in their place well even if students interfere with them. We are using double convex lenses to create collimated light, with the more bulbous side of the lenses facing towards the fluid. Using this orientation will decrease warpage around the edge of the final image. Lenses also have focal lengths that must be taken into consideration. The shorter a focal length, the more important it is for the light to be a point source.

At first, we were using lenses that were scratched and too small for our purposes. We want lenses that would clearly show the area in which the shock wave would be without question. This led to the purchase of lenses with about 43mm focal lengths and 46mm diameters. **Figure IX-3** shows the area in which the viewer would see the shock wave.

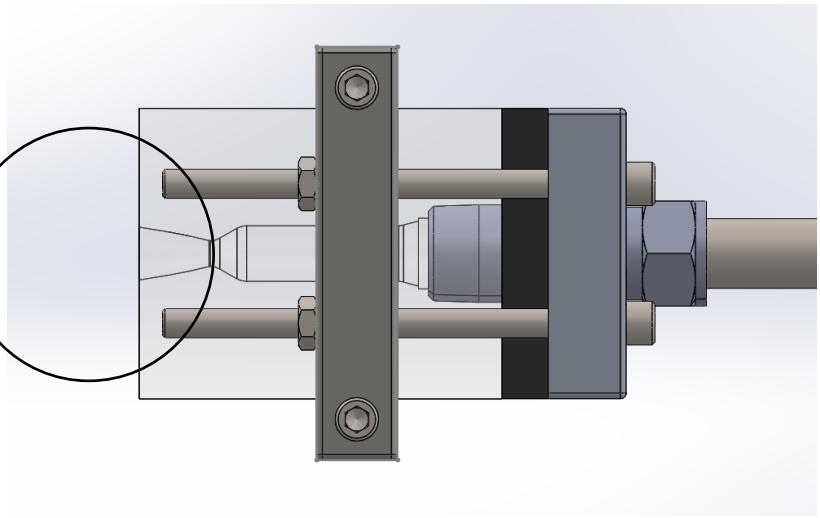

***Figure IX-3**: Viewing Radius*

As for placement on the rail, the distance between the two lenses is negligible for our purpose if the light and the knife edge are placed a focal distance away from the lenses on either side as shown in **Figure IX-4**. If the components are not placed correctly relative to each other, the image will be blurry.

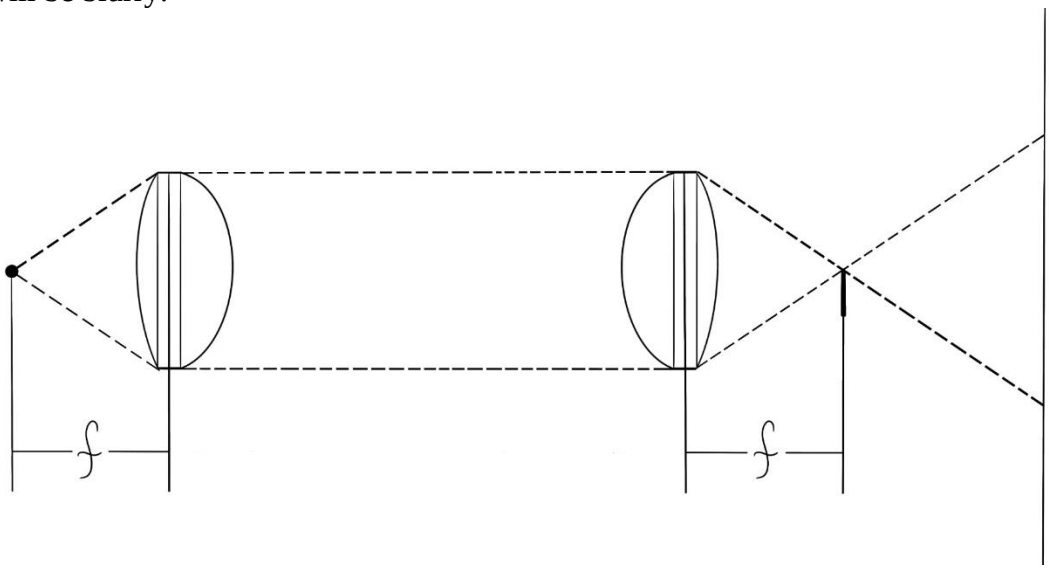

***Figure IX-4**: Diagram indicating focal length*

Each component must have a protective housing. We designed the table to withstand students sitting or even standing on it with the tank to make sure no one could be hurt. Likewise, the optical mounts need to withstand students' curiosity. To hold the lens to the rail, we created the mount shown in **Figure IX-5**.

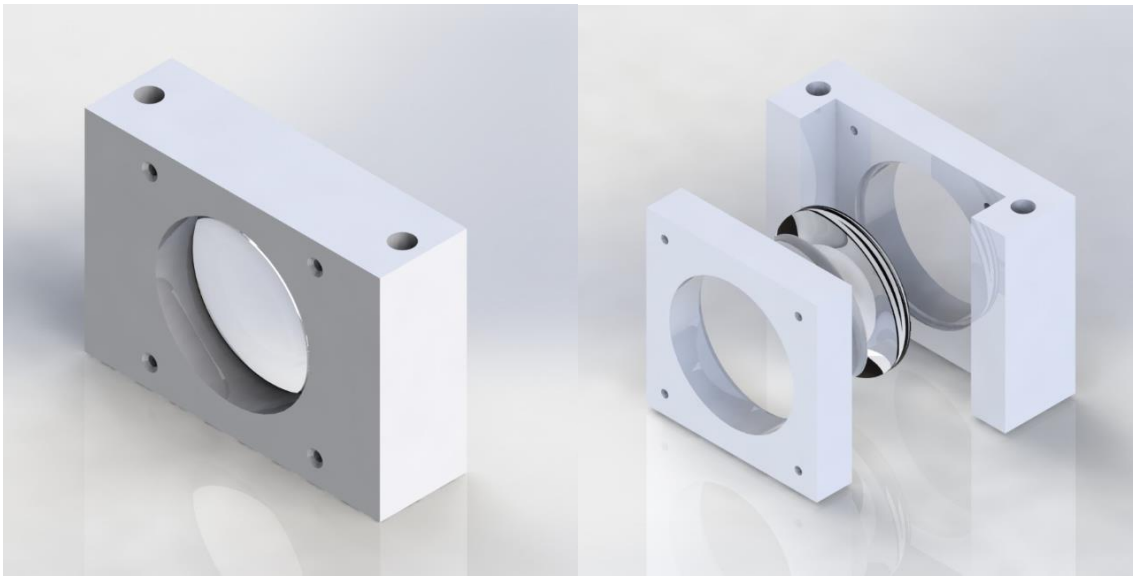

***Figure IX-5**: Lens Mount Design*

This mount design was 3D printed on Walla Walla University's UV resin printer to ensure the longevity of this part. Using resin vs FDM was also helpful because the lens mount had holes in different axis and needed precision on the circles that would hold the lens. FDM may have warped holes that were not directly on the printing bed and would not have been as precise. Once they were printed, holes were taped into the back part and four machine screws were used to hold the two parts together. Tissue paper was used to cushion the lens in the mount. Two holes were also tapped into the sides to allow for a set screw. We need motion to be able to raise or lower the lens if needed, but once it is in the right position, it needs to stay there. For this we used $1/4^{th}$ – 20 machine screws as set screws to keep the fastener from striping the plastic threads. This prosses was repeated for both lenses. Below in **Figure IX-6** of the completed part.

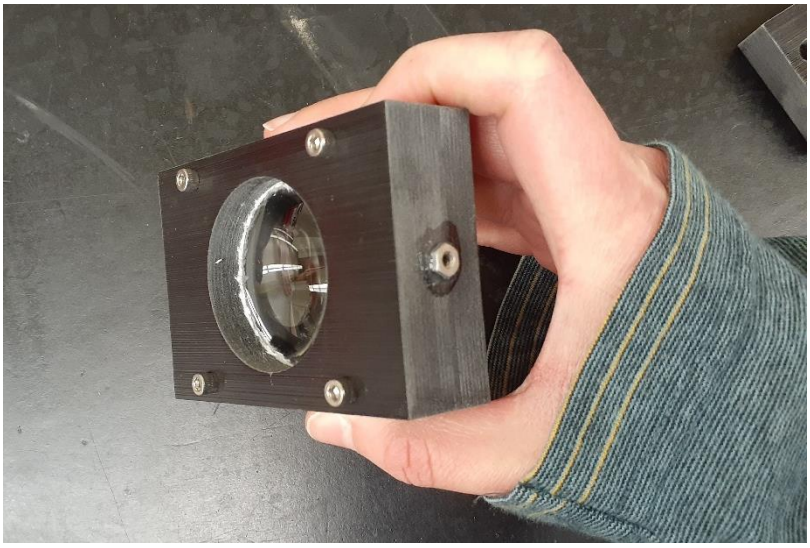

***Figure IX-6**: Lens mount*

C. Camera Selection

During testing, we found that the camera needed to be very close to the knife edge. To make sure the camera is close to the knife edge in the final design, the camera housing will include the knife edge. The current camera connects via USB to a computer and acts just like a webcam. Using a program called AMCap, we were able to adjust exposure for a well-balanced image. The software development portion of this project will be work with the software side of the camera and synchronize it with the data gathered from the pressure and temperature instrumentation.

D. System Mounting

Several iterations of mounting designs have been discussed to lift the schlieren imager to the height of the nozzle and make sure the system is adjustable. Below, **Figure IX-7**, shows our preliminary designs in solid works.

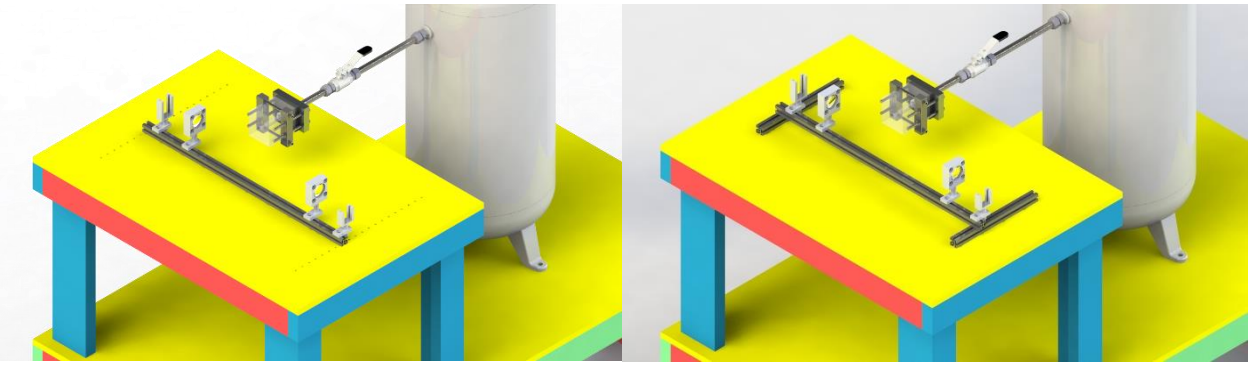

***Figure IX-7**: Preliminary Mount Designs*

We decided to settle on the mounting shown **Figure IX-8**. The thick railing keeps the whole system stable and free of rotation. Our intention was to build the optical table tall enough so that the rail would be just below the nozzle. However, we build the table to short. This played into our favor because it will allow for more versatile mounting in the future if needed. To get the main rail to the correct height, short, extruded aluminum rail was used as feet on both sides and the supporting rail that allows for forward and backward movement was also very tall. Between these two adjustments, the main rail was brought to the correct height. There is enough room for minor adjustments in the optical elements, but not so much space that the gap is unreasonable.

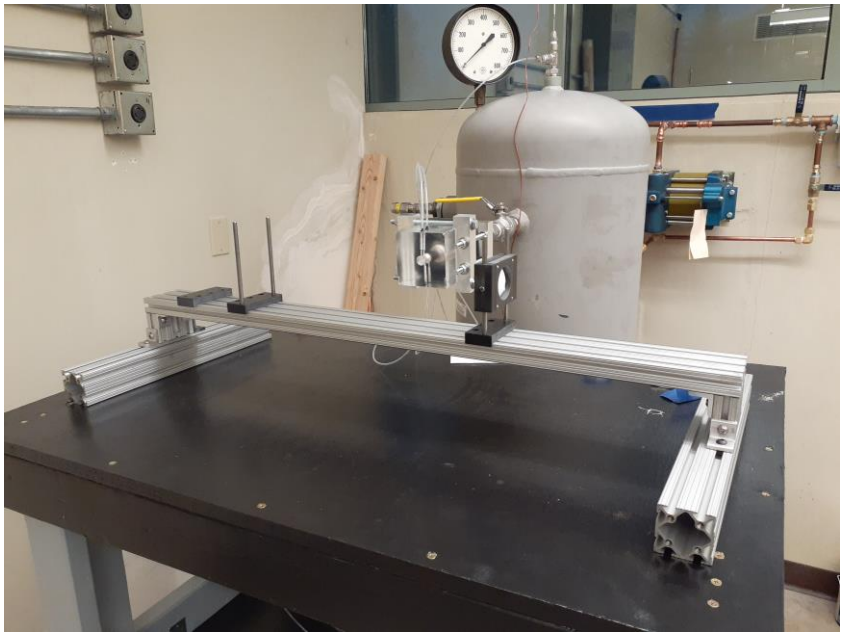

***Figure IX-8**: Final rail design*

To connect each element to rail, a slider is required. The purpose of this is to allow for left and right adjustment on the rail, and to allow each element to raise or lower. Fasteners connect the 3D printed base into the rail and steel ¼" rods were cut, rounded, and glued into holes shown on the left side of **Figure IX-9**. From there, each element will slide on and be held with set screws shown on the right side of **Figure IX-9**.

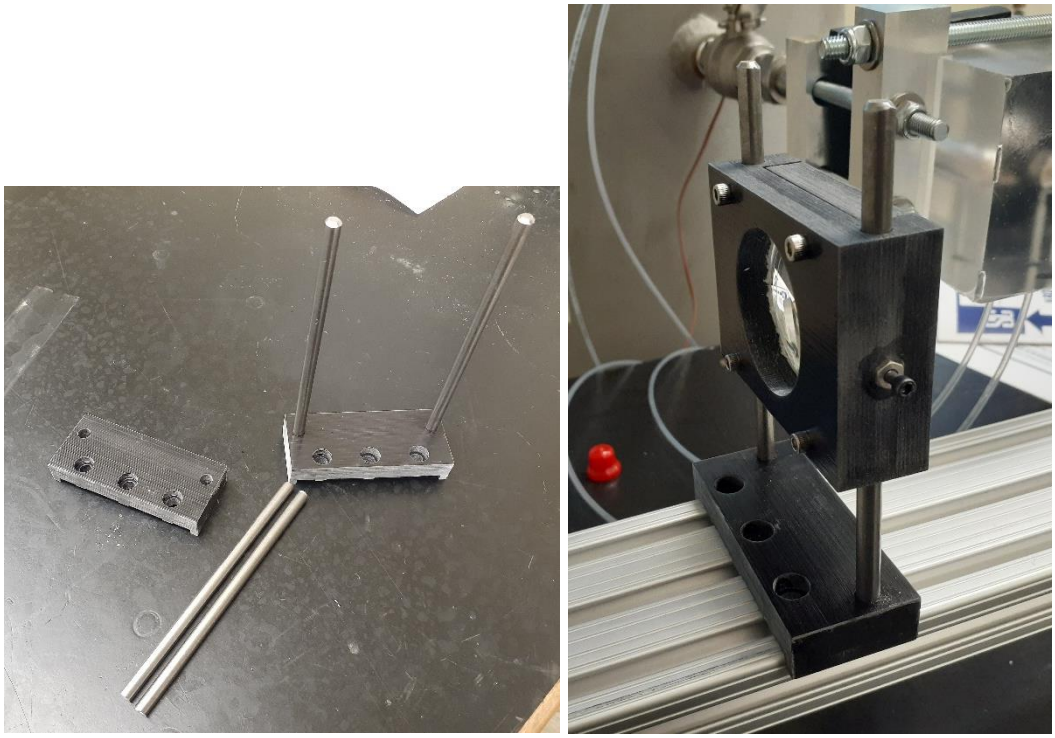

***Figure IX-9**: Slider assembly and use*

E. Testing

We have been able to do some testing even with the setbacks we faced. Our goal was to show the shock wave being produced and we were able to see one! In **Figure IX-10**, the hard edge on the left side coming out of the nozzle is the beginning of a shock wave. We expect this to become more prominent and extend farther at higher pressures.

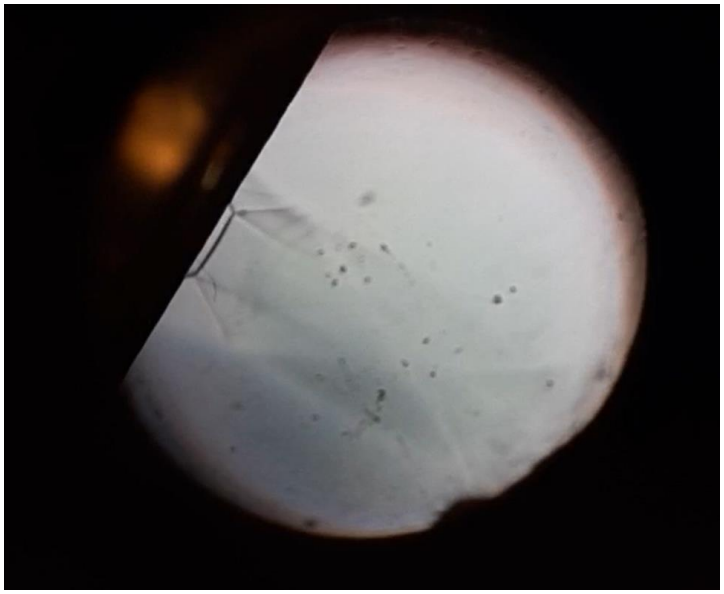

***Figure IX-10**: Shock wave at 150psi*

X. Pressure and Temperature Instrumentation

To truly gain an understanding of supersonic flow from a laboratory experiment, both pressure measurements at various locations in the nozzle as well as pressure and temperature measurements in the tank are necessary. This way, students can study the compressible flow equations they learn in Fluid Mechanics class and see if the data gathered agrees with these equations. This is the motivation behind implementing a pressure and temperature instrumentation system on the nozzle and the tank of the supersonic nozzle experimental apparatus.

To implement the instrumentation system, the first step was to use the compressible flow equations to predict pressures throughout the nozzle. Using this information and a constraint on maximum error, pressure sensors for the nozzle were carefully selected to meet the needs of the system. The same was done for the pressure and temperature sensors to be installed on the tank itself. A system of fittings was also designed to allow the connection of these sensors to the tank. Next, holes were designed for the nozzle to allow the insertion of the high-pressure tubing from which the pressure sensors would measure the pressure in the nozzle. After careful consideration, these holes were machined precisely into the nozzle.

Now that the connection between the sensors and the experimental apparatus was well-understood and mostly complete, the connection between the sensors and the computer that would process the data was designed. More specifically, the pressure sensors required an excitation voltage to run, as well as amplification in order to be easily readable by the analog-to-digital converter (ADC). This was accomplished through a set of amplifier modules, which are to

be connected to the sensors on the input side and the ADC on the output side. The ADC will be used by the computer to read the data and interpret it as needed.

A. Supersonic Flow Calculations

The first task in this division of the project was to calculate expected properties at each location of interest within the nozzle. This was critical because pressure ranges needed to be known to select and purchase pressure sensors. To do this, it was important to decide at which locations pressure should be measured in the nozzle. Location in a converging-diverging nozzle, at least as far as compressible flow calculations are concerned, is determined by the cross-sectional area. Different cross-sectional areas indicate different locations within the nozzle. As a result, five cross-sectional areas were chosen as locations of study. One was an area of 0.283 square inches upstream of the nozzle throat, three at areas of 0.102 square inches, 0.152 square inches, and 0.212 square inches were downstream of the throat, and one was at the throat with an area of 0.062 square inches. This provided a good spread of locations at which to measure pressure.

Once the desired locations were decided, the specific times that pressure would be calculated at needed to be chosen. Because tank pressure is what really changes over time during the experiment, pressures of 600, 300, 100, 50, 30, 20, and 14.7 psi were chosen because they proved to provide a good spread of data. With these pressures chosen, the process of finding the pressure and other properties at each point needed to be repeated 35 times. As a result, a software package was written in Python, using the method described in the following section to calculate properties at each point.

1. Method for Finding Properties at a Single Location

Though all properties can be obtained at any point in the nozzle in the same way, the following paragraphs will describe just how pressure is found, since it is the property of interest. In order to find pressure at an arbitrary location in the nozzle, knowns, unknowns, and assumptions must be listed. As has been described before, the area at the target location will always be known, at least as approximated by the ideal CAD model of the nozzle, and the same is true of the area at the throat. Since pressure in the tank has been chosen to correspond with different times, this value will also be known each time. Additionally, the pressure at the exit of the nozzle should always be atmospheric as long as a shockwave is inside the nozzle. If it is not, then the exit pressure is not a required value for the calculation due to the nature of the compressible flow equations. However, the location of the shockwave, indicated by area, is unknown, as well as the pressure at the target location.

Known:	**Assumptions:**
Area at target location (A)	Adiabatic Flow
Area at throat (A^*)	Isentropic Flow
Pressure in the tank (P_0)	1-Dimensional Flow
Pressure at the exit (P_e)	

Unknown:

Area of shockwave location (A_{shock})

Properties at target location (P)

***Figure X-1**: Knowns, unknowns, and assumptions for compressible flow calculations*

The simplest, most common model for analyzing compressible flow makes a number of key assumptions, shown in **Figure X-1**. First, it assumes adiabatic flow, meaning that no heat is lost or gained across the walls of the nozzle. Under the time scale of this experiment, this has been deemed an appropriate assumption. Also, the model assumes isentropic flow. This assumption technically includes the adiabatic assumption, but also means that the flow has no frictional losses to the walls. Finally, the flow is assumed to be one-dimensional, meaning that at each location within the nozzle, all properties are uniform across the cross-sectional area. All three of these assumptions were deemed acceptable for this experiment, and so this model was used to theoretically calculate pressures and other properties at each location within the nozzle. Specifically, the formulation of this model provided in Frank White's *Fluid Mechanics* textbook was used for the analysis (White, Frank M. 2016, 593-626).

Before worrying about the location of the shockwave, it is helpful to first devise a method by which, absent a shockwave, pressure and other properties can be found throughout the nozzle. This can be done using the equations in **Figure X-2**. Considering that the pressure in the tank, the throat area, and the target area are always known, the Area-Mach Number Relation can be used to find the Mach number of the flow at any location. Note that this equation can yield two separate answers, one that is supersonic and one that is subsonic. If a shockwave is not present, the subsonic value will always be the correct one. Once Mach number is known, the Mach Number Relation can be used to find the pressure at any point. Other equations exist that parallel this relation for other properties as well.

Area-Mach Number Relation:
$$\frac{A}{A^*} = \frac{1}{M_a}\left[\left(\frac{2}{k+1}\right)\left(1+\frac{k-1}{2}M_a^2\right)\right]^{(k+1)/[2(k-1)]}$$

Mach Number Relation:
$$\frac{P_0}{P} = \left(1+\frac{k-1}{2}M_a^2\right)^{k/(k-1)}$$

***Figure X-2**: Basic compressible flow equations*

While this method works for finding pressures of locations in the nozzle when normal shockwaves are not present, it does not cover the case where a shockwave is present within the nozzle. The first thing that changes if a shockwave is present is that, when finding pressures at

points upstream of the shockwave but downstream of the throat, the supersonic value yielded by the Area-Mach Number Relation is the correct one, while positions upstream of the throat are still subsonic. The second thing that changes is that, while the previously mentioned equations also function downstream of the shockwave, they do not apply when moving from one side of the shockwave to the other.

To find properties on the downstream side of the shockwave given properties on the upstream side of the shockwave, the three Normal Shock Equations, included in **Figure X-3**, must be used. It is important to note that, after crossing a normal shock wave, the throat area used in calculations will no longer be the actual area of the throat but must be adjusted based on the physics that occurs during that transition, since it is not isentropic. By using the Normal Shock Equations, this new critical area can be found, along with the Mach number and pressure on the downstream side of the shock wave. Of course, these equations require already knowing these properties on the upstream side of the shockwave, which can be found through the method previously mentioned.

Normal Shock Equations:

Mach Number: $$Ma_2^2 = \frac{(k-1)Ma_1^2+2}{2kMa_1^2+2}$$

Pressure: $$\frac{P_2}{P_1} = \frac{1}{k+1}[2kMa_1^2 - (k-1)]$$

Critical Area: $$\frac{A_2^*}{A_1^*} = \left[\frac{2+(k-1)Ma_1^2}{2+(k-1)Ma_2^2}\right]$$

***Figure X-3**: Normal shockwave equations*

So far, a method has been described for finding pressure at any point within the nozzle if there is no shockwave, or if the shockwave location is known. However, only three of the four initially known values for each point have been used, and one of the unknown values, the location of the shockwave, has been assumed to be known. To find the location of the shockwave, the equations above must be used slightly differently, using the known atmospheric pressure at the exit and working backwards to find what the tank pressure would need to be to cause that exit pressure. More specifically, this process must be carried out for two separate cases: a normal shockwave at the throat of the nozzle, and a normal shockwave at the exit of the nozzle. If the current tank pressure at the time we are measuring is above the expected tank pressure when there is a normal shockwave at the exit, then all points downstream of the throat will be supersonic, with no shockwave in the nozzle. If the current tank pressure is instead below the expected tank pressure when there is a normal shockwave at the throat of the nozzle, then all points downstream of the throat will be subsonic. However, if the current tank pressure is between these two limiting cases, a normal shockwave is present at some place within the nozzle, and the solution becomes much more difficult. First, the normal shockwave must be located, and only then can the pressure at the point of interest be found.

When a normal shockwave is present in the nozzle, this method for finding pressure at a specific point must be used to locate that shockwave. Once the shockwave is located, this method can be applied again to find the pressure at the point of interest. However, because the normal shockwave location is unknown, it must remain as a variable within the equation in order to solve for it. Additionally, when searching for the shockwave, the equations must be solved for pressure specifically at the exit, which is known to be atmospheric. Thus, the entire system of equations will have only a single unknown that is relevant to the problem: the cross-sectional

area of the shockwave. This is not easily solvable by hand, and two methods exist with which the problem could be solved. The first approach would be to guess normal shockwave locations until the exit pressure matches the atmosphere. This would be much faster for the calculation of a single point with a known tank pressure and location. However, it becomes incredibly tedious when calculating a large number of points. The second approach would be to combine this entire process into a function in a computer program, and then use an optimization package to solve the system of equations for the area of the shockwave. This method is much more difficult to implement when solving for a single point, but when solving for a variety of points, it is much swifter. The second approach was chosen for this project and was implemented in the form of a software package.

2. Structure of Python Software Package

Python was the language chosen to implement the previously described solution method. A variety of libraries made for computing with Python were used in this process. The first and most important of these libraries was numerical Python, or NumPy for short. NumPy allows python to take on many of the tasks traditionally solved by MATLAB, including creating and manipulating arrays. The matplotlib library was used to plot results as necessary, in order to allow the data calculated to be analyzed visually. SciPy's optimization library was used to solve equations, and a library called pandas was also used to allow data to be easily exported into Excel. I also programmed my own small library to convert key values between the metric and imperial system, to allow inputs and outputs of either system.

Armed with these tools, a software package was programmed to calculate properties within converging-diverging nozzles according to the method described in the previous section. Using this package, the pressures in the nozzle at the locations and tank pressures specified were calculated using this method. The entire software package is too large to include in this paper. However, the code which makes use of the software package to calculate the data is included in **Appendix B: Python Code for Calculating Supersonic Flow Properties**. The data, in polished form, is displayed in **Table X-1**.

***Table X-1**: Theoretical pressure, calculated using the python software package based on the compressible flow equations*

Pressure (psia)						
		Cross-sectional Area (in^2)				
		0.283	0.064	0.102	0.152	0.212
Tank Pressure (psia)	600	593.25	237.34	79.70	39.20	22.64
	300	296.62	118.67	39.85	19.60	11.32
	100	98.87	39.56	13.28	6.53	3.77
	50.0	49.44	19.78	6.64	3.27	1.89
	30.0	29.66	11.87	3.99	1.96	14.29
	20.0	19.77	7.91	12.22	13.96	14.53
	14.7	14.53	9.69	13.30	14.11	14.40

B. Nozzle Sensor Selection

The second task in this division of the project was to select the pressure sensors to be connected to the nozzle. The purpose of the sensors is to measure the pressure in the nozzle at each cross-sectional location specified in the previous section over time. As a result, each sensor needed to be selected to have the proper pressure range based on the expected pressure ranges over those points. Using the data calculated in the previous section, pressure ranges were easily estimable at each point by making note of the highest and lowest pressures present there over time. For example, at a cross-sectional area of 0.062 square inches, the highest pressure present is 316.97 psia, while the lowest is 7.77 psia. As a result, an absolute pressure sensor with a range somewhat larger than 0-320 psia is needed to measure that point.

In addition to pressure range, each sensor also needed to be accurate, so the data collected would reflect the compressible flow model enough to be recognizable. After much consideration, it was decided that each sensor needed to have an error of no more than 10 percent of the smallest expected reading. Because sensors on the market often provide error as percent full-scale reading, the following equation was used to convert between the two. The variables in this equation are percent smallest expected reading ($\%SER$), percent full-scale reading ($\%FSO$), maximum reading specified for the sensor (P_{max}), and minimum reading expected based on calculations discussed previously (P_{min}).

$$\%SER = \%FSO \cdot \frac{P_{max}}{P_{min}}$$

A variety of pressure sensors were researched and checked to see if they had the proper ranges with a relatively low %FSO at a decent cost. This narrowed the search down to three sensors. Then, each sensor was tested for whether it met the accuracy requirements specified previously. The results of this analysis can be found in **Table X-2**. As can be seen, three $220.00 sensors and two $309.70 sensors were deemed necessary.

***Table X-2**: Evaluation results comparing various pressure sensors based on accuracy*

	$60 Sensor (0.50% FSO Error)	$220 Sensor (0.25% FSO Error)	$309.7 Sensor (0.10% FSO Error)
	Pressure Ratings (psi)		
Sensor 1	725	1000	1000
Sensor 2	725	500	500
Sensor 3	145	100	100
Sensor 4	72	50	50
Sensor 5	29	50	50

Both selected sensors were actually the same sensor, with the more expensive one containing an upgrade for increased accuracy. The sensor of interest was the Druck UNIK 5000 series sensor, which can be ordered with a variety of pressure ranges. The details of this sensor

are described in a later section. An image of the sensor is depicted in **Appendix C: Data Acquisition System Components**.

C. Tank Sensor Selection

In addition to measuring the temperature in the nozzle, it was also important to measure pressure and temperature in the tank, since these values are necessary to examine if the compressible flow equations describe the experiment properly. Before selecting specific sensors for the tank, it was first necessary to determine exactly how the sensors will be connected to the tank. Ultimately, a reducer will be used to attach a tee to the top of the tank. Then, a tube to carry the pressure in the tank to the pressure sensor will be attached to the side of the tee using a Swagelok Tube Fitting, a type of fitting that can permanently attach to any cylindrical surface of a given size. A similar fitting will be used to connect the tee to a long, sheathed thermocouple, which will penetrate straight through the fittings into the tank. A schematic is included in **Figure X-4** to aid in understanding this setup.

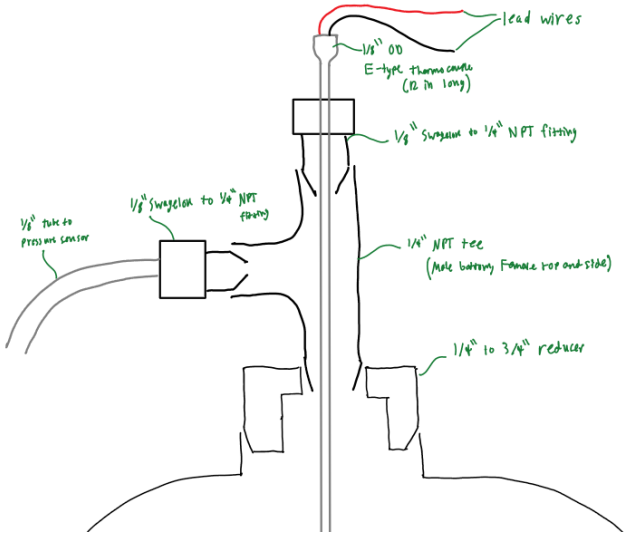

***Figure X-4**: A schematic of the pressure and temperature measurement system for the tank*

After deciding on this setup, a pressure sensor and sheathed thermocouple were selected. For consistency, another Druck UNIK 5000 pressure sensor without upgraded accuracy was chosen to measure pressure in the tank. An additional bonus to this sensor was that a tube could easily be attached to it using another Swagelok Tube Fitting. For the thermocouple, a temperature range had to be calculated before selection. This only required finding the maximum possible temperature of air emerging from the booster pump into the tank, since the lowest possible temperature in the tank would simply be room temperature. Assuming isentropic compression, which would result in the theoretical maximum outlet temperature of compressing air from 120 psia to 600 psia in the booster pump, the following isentropic relation from White's *Fluid Mechanics* textbook was used, assuming room temperature on the low-pressure side of the booster pump (White, Frank M. 2016, 597):

$$\frac{P_2}{P_1} = \left(\frac{T_2}{T_1}\right)^{\frac{k}{k-1}}$$

This calculation resulted in a maximum temperature of 191 degrees Celsius, which is about 376 degrees Fahrenheit. Using room temperature and this temperature as an appropriate range, a sheathed type-E thermocouple was selected from Omega for use in this application.

D. Nozzle Tap Design and Implementation

The next task that had to be accomplished in this division of the project was the design and implementation of nozzle taps, or holes drilled into the nozzle to allow the tubes to be connected to the nozzle on one end and to the pressure sensors on the other end. As discussed for connecting the pressure sensor to the tank, each of the Druck UNIK 5000 pressure sensors can be connected to a tube using a Swagelok Tube Fitting. As a result, only the connection of the tubes to the nozzle had to be designed manually. As for the tubing, a 50-foot-long spool of 1/8 inch outer diameter tubing rated to withstand over 600 psi of pressure was purchased from McMaster Carr.

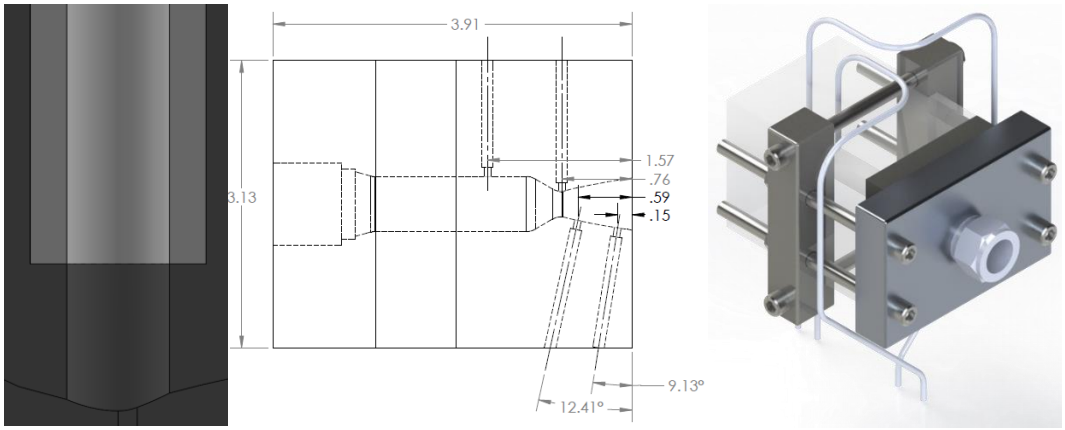

Figure X-5*: Images, from left to right, of what types of holes were drilled (a), how exactly those holes were placed in the nozzle (b), and how the completed design should look (c).*

In creating holes for the tubing to slide into the nozzle, a variety of factors had to be considered. First, changes in cross-sectional area needed to be minimized between the hole emerging on the inner surface of the nozzle and the inner diameter of the tube itself, to avoid resonant frequencies creating whistler tones, adding noise to the pressure readings. Second, it was important to keep the tubing from protruding into the inside area of the nozzle, to avoid altering the flow field and thus pressures within the nozzle. Third, the holes needed to be drilled so as to emerge on the inner surface of the nozzle normal to the nozzle surface, to avoid air rushing up the holes, adding their dynamic pressfure to the static pressure being measured and invalidating the reading. Finally, the holes needed to be drilled a reasonable distance from one another so that small mistakes in machining would not result in overlapping any of the holes, which would ruin the nozzle. As a result of all these considerations, the holes were drilled in two stages, as seen in **Figure X-5a.** First, a hole the same size as the inner diameter of the tubing was drilled normal to the inner surface at the location desired. Second, a hole the same size as the inner diameter of the tubing was drilled at an offset to the surface. As a result, the tube can slide up to a shoulder in the nozzle, avoiding protrusions into the flow field in addition to eliminating any changes in cross-sectional area. The tube will be secured to the nozzle by gluing it to a washer, and then gluing the washer to the nozzle. **Figure X-5b** shows the angles at which these holes were drilled into the nozzle. The holes were drilled perpendicular to the surface of the

nozzle, as planned. However, to ensure that the holes were not too close to each other, one of the desired locations of pressure measurement had to be sacrificed, resulting in only four locations in the nozzle where pressure could be measured. This is disappointing but should still be more than satisfactory in studying the supersonic flow phenomena that will occur in this experiment. **Figure X-5c** shows how the design should look when finished.

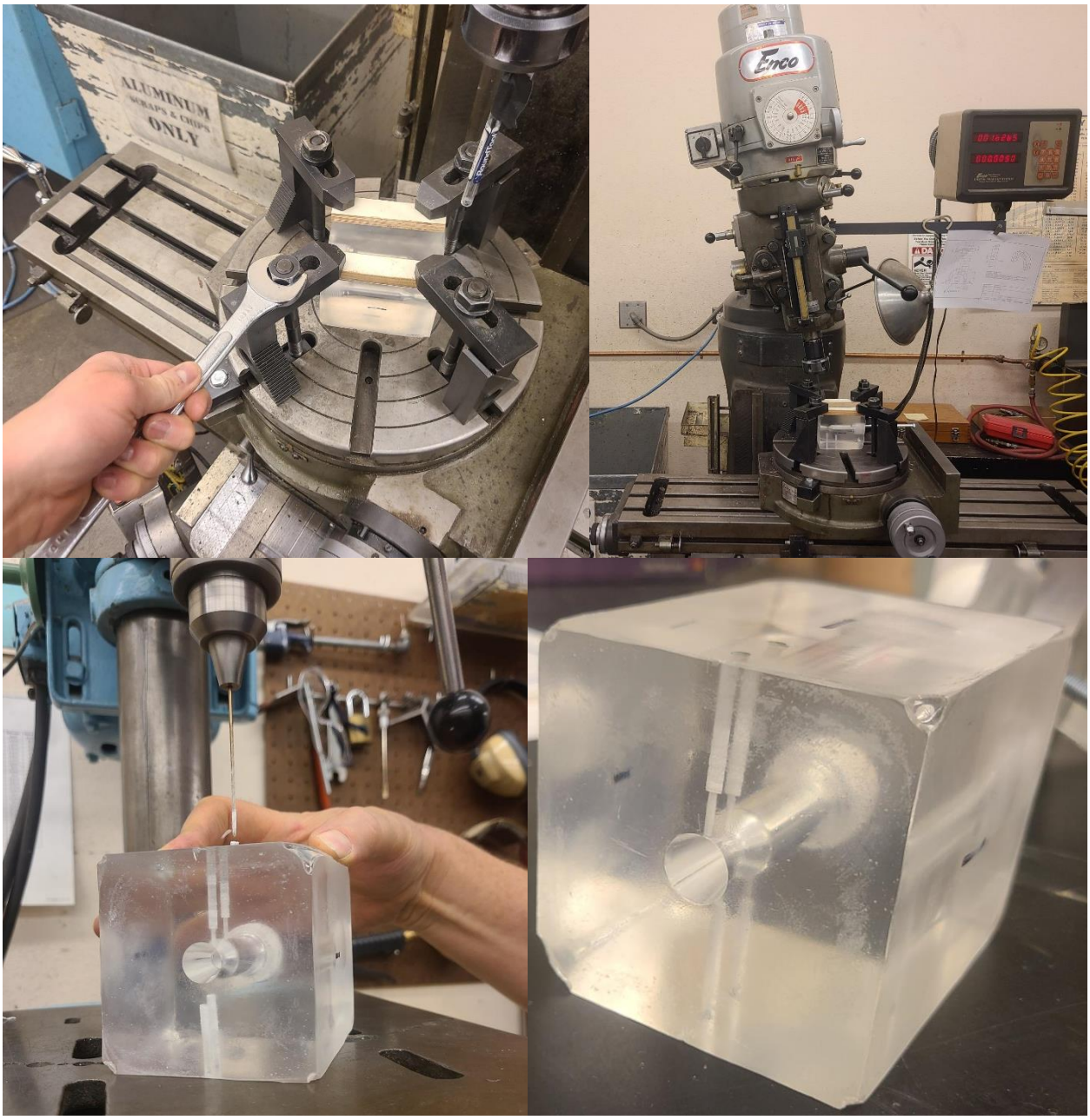

Figure X-6*: Images, from left to right, of clamping the nozzle in place on the mill (a), drilling the larger holes at an angle using the mill (b), drilling the smaller holes to the surface of the nozzle (c), and the nozzle with all the holes drilled in it (d).*

With the design complete, the holes were drilled into the nozzle using a mill and a drill press. More specifically, the nozzle was clamped to a rotary table on a mill, as shown in **Figure X-6a**. Then, the mill was tilted, and the larger holes were drilled at an offset from the inner

surface of the nozzle at precisely the correct locations using the LCD on the mill in conjunction with the engineering drawings of the desired holes displayed previously. This part of the process is shown in **Figure X-6b**. Once these holes were drilled, a piece of the tubing was inserted into each hole, and a drill press was used to drill the smaller holes all the way through to the surface of the nozzle, as shown in **Figure X-6c**. The final product, shown in **Figure X-6d**, turned out very nicely. This process was followed to drill holes in the spare nozzle as well.

E. Data Acquisition System Design and Implementation

The fifth task that had to be completed for this division of the project was to design and implement a data acquisition system, or a system that can take the data output by the pressure sensors into a digital format that a computer can manipulate. This required procurement of a variety of components.

Because the pressure sensors output an electrical signal, an analog-to-digital converter (ADC), a device capable of taking analog electrical signals and providing them to a computer in digital format, was necessary. We chose to use a Labjack UE-9 Pro, an ADC that had already been used previously for a similar experiment in the Fluid Mechanics Laboratory. This device is capable of taking analog voltage inputs from -5 to 5 DC volts and providing them to a computer in digital format.

The Druck UNIK 5000 pressure sensors selected have four electrical connections that must all be used for the sensor to function properly. Two of these connections must be used to provide the sensors with a steady voltage source of around 10 DC volts, and the other two produce a voltage between 0-100 DC millivolts depending on the pressure experienced by the sensor, allowing pressure to be measured in the form of voltage. This produced two new requirements that had to be met for the data to be converted into digital format. First, the sensors needed a voltage source that would provide them with a steady 10 DC volts. Second, the ADC required input on the order of 5 DC volts, not 100 DC millivolts. As a result, an amplifier was also required to rectify this problem. Both of these requirements were met using an industrial signal conditioning package.

The industrial signal conditioning package consists of eight distinct components. First, five Dataforth SCM5B38-07 strain-gage signal conditioning modules were needed, one for each pressure sensor. These modules supply a steady excitation voltage of 10 DC volts, while also amplifying the output signal of the sensors, multiplying the voltage to be 5 DC volts for every 100 DC millivolts. Second, one Dataforth SCM5B47E-08 linearized type-E thermocouple signal conditioning module was needed and serves much the same purpose as the other modules, only for the thermocouple instead of the pressure sensors. Third, a single SCMXPRT-001 5 DC volt power supply was necessary to provide the signal conditioning modules with power to amplify the signals from the sensors. Finally, a single Dataforth SCMPB05 non-multiplexed eight channel back panel with cold-junction compensation was needed. This piece of equipment simply takes the power from the power supply and distributes it to the signal conditioning modules, as well as providing screw terminals to easily connect to the inputs and outputs of these modules. With these eight components, the signal conditioning package is capable of powering the pressure sensors and amplifying the outputs of both the pressure sensors and the thermocouple to a range readable by the Labjack UE9-Pro ADC.

Measurement of pressure and temperature follows a straightforward progression. The pressure originates in the nozzle of the tank and is transmitted through the tubes to the pressure sensors. The data is then transmitted to the industrial signal conditioning package. The

temperature originates in the tank and is transmitted as an electrical signal to the industrial signal conditioning package as well. The pressure sensors are also powered by the industrial signal conditioning package. Once all of the data has been transmitted to the signal conditioning package, it is amplified and outputted to the ADC, to be recorded and manipulated by the computer. Images of each of these components are included in **Appendix C: Data Acquisition System Components**.

Figure X-7*: Fully Assembled Data-Acquisition System*

All these components, as well as the sensors themselves, also needed to be mounted close to each other to allow ease of use and testing. More specifically, they needed to be mounted to the table holding the tank to avoid incredibly long lengths of tubing. This was accomplished by measuring all the components and cutting a plywood board to a size that could comfortably fit them all. This board was then painted carefully, and the components were screwed to the board at right angles from the edges. Additionally, a shield needed to be attached to the board to prevent stray water particles in the Fluid Mechanics Laboratory from frequently landing on the electronics. To accomplish this, a sheet of plexiglass was cut and bent using a wooden mold and a heat gun to match the shape of the board. Then, an indentation was cut into the bottom of the plywood board, and two acrylic hinges were attached to the plexiglass shield using strong adhesive and to the board using both adhesive and a couple wood screws. A picture of this assembly without any of the electronics screwed to it is included in **Appendix C: Data Acquisition System Components.** The electronics have since been attached, as shown in **Figure X-7**.

Once all of the components were in place, the entire system had to be connected. First, all the connections between the pieces of the data acquisition system were connected. This involved gluing washers to each tube, and then using those to glue the tubes to the nozzle to secure them in their slots. The results of these efforts are shown in **Figure X-8**. Additionally, these high-pressure tubes were connected to the pressure sensors using Swagelok tube fittings. The thermocouple and one of the pressure tubes was also attached to the tank as described previously, and the thermocouple was connected to the signal-conditioning backplane using a type E thermocouple extension cord.

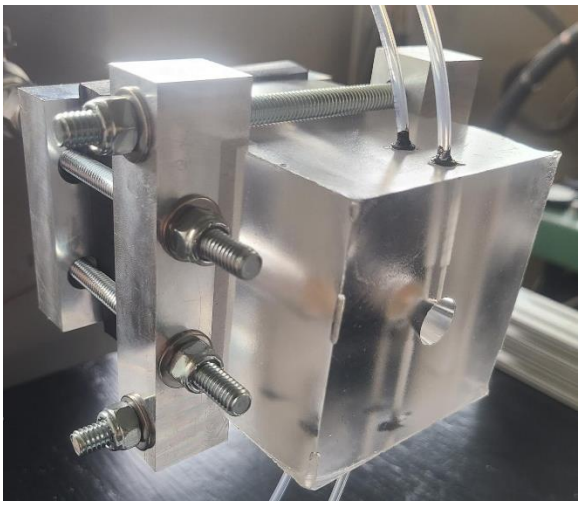

***Figure X-8**: Final Instrumented Nozzle*

F. Pressure Sensor Testing

With everything connected as much as possible, the next step was to test the pressure sensors. After some investigation, it was discovered that the UNIK 5000 sensors selected for this project are the most accurate pressure sensors in the laboratory except for the barometer on the wall, which only measures atmospheric pressure. After a little bit of preliminary testing, a few conclusions were drawn about the pressure instrumentation as a system. First, the pressure sensors themselves had already been calibrated, and proved to have reliable gains and offsets. However, the amplifier modules were not so reliable. While their gains were indisputable, their offsets left much to be desired, staying constant within a test session but changing between sessions. As a result, a calibration routine was developed using the wall barometer in order to calculate these offsets each time the experiment is run.

The calibration routine goes as follows. First, the sensor gains and offsets, along with the amplifier gains, are retrieved for use in the calibration routine. Next, the atmospheric pressure in the laboratory is read from the wall barometer. This data is then used to calculate the linear offset of the amplifiers, allowing pressure to be read accurately from each sensor. These steps and the exact equations used in this procedure are included in **Figure X-9**. The calibration procedure was useful for testing, but it is also incorporated in the software created in the **Custom Software Package** section of this paper, allowing calibration to be completed automatically each time the experiment is run, with only the barometer pressure needing to be input each time.

Once the sensors were calibrated properly, they were ready to be tested for accuracy. Due to their superior accuracy, the best way to test them as actually to compare their reading of the same pressure at unknown tank conditions. To do this, the sensors were hooked up to the tank two at a time, and then the tank was pressurized to an unknown pressure. Then, the voltages of the sensors were read and used to calculate pressure using the formulas in **Figure X-9**. The results of these tests for each set of sensors are displayed in **Table X-3**.

From **Table X-3**, it is clear that the sensors functioned superbly. The safety factor percentage displayed is the expected error in the readings over the actual difference between the readings and shows that the sensors are function well within the capabilities required of this application.

Procedure:

1. Permanently store amplifier gains, as well as sensor gains and sensor offset, in the software
2. When booting up, have the user input the barometer pressure reading and click "Recalibrate"
3. Have the Labjack sample amplifier output readings at that time, and then calculate amplifier offset using the below formula.

P_{atm} = Barometer pressure reading (psi)
V = Amplifier output reading (V)
m_a = Amplifier gain (V/mV)
b_a = Amplifier offset (V)
m_s = Sensor gain (mV/psi)
b_s = Sensor offset (mV)

$$b_a = m_a\left(\frac{V}{m_a} - (m_s P_{atm} + b_s)\right)$$

4. Now pressures can be calculated, using the following formula, for each amplifier, at each point in time.

$$P = \frac{\frac{V - b_a}{m_a} - b_s}{m_s}$$

***Figure X-9**: Calibration procedure for the pressure instrumentation system*

***Table X-3**: Pressure sensor data from testing them against each other*

Sensor	V (V)	P (psi)	Delta P (psi)	Safety Factor
1	4.32	43.163	0.174	
2	2.141	43.337		61%
2	2.141	43.337	0.000	
3	0.424	43.337		290549%
3	0.424	43.337	0.069	
4	0.212	43.406		2210%
4	0.212	43.406	0.133	
5	0.206	43.272		960%

G. Thermocouple Testing

Finally, the thermocouple needed to be tested to ensure that it too was functioning within expectations. In order to do this, the gain and offset of the thermocouple linearization and amplifier module was obtained from manufacturer. Then, the thermocouple was submerged in ice water and then in boiling water, with its voltage recorded each time and then converted into an expected temperature. Then, the boiling and freezing point of water was obtained for the elevation of Walla Walla University and was compared to the reading. The result was very good, resulting in a maximum of 0.37% error. After that, the thermocouple was tested against a temperature sensor in the laboratory and was found to have a reading that was off by about 1.8 degrees Celsius. However, after further thought, this made sense, since this thermocouple is also the best temperature sensor in the lab, indicating that this error likely came from the temperature sensor it was being tested against, not the thermocouple itself. As a result, the thermocouple was deemed to be adequate for our purposes. This data is tabulated in **Table X-4**.

Table X-4*:Thermocouple test results at a handful of temperatures*

	T (°C)	Error (°C)	Error (%)
Ice Bath	0	0	0.00%
Boil	98.8	0.37	0.37%
Fluid's Lab	20.2	1.8	8.18%

Almost everything that was planned for this project section was completed. All that remains is to attach all of the outputs of the amplifier modules to the ADC, a task that will be undergone once the custom software package is fully finished.

XI. Custom Software Package

A. Introduction to Software Design Aspect

In order to create a meaningful lab experience, a custom software package was necessary. The software reads raw data from the physical instrumentation system and optical instrumentation camera, processes it, and displays it in a visually appealing and comprehensible manner. At a high level, the software has four main objectives: display live video feed, provide live pressure and temperature data, record and save live sessions for later replay, and provide an option to export sensor data in a user-friendly format for further processing and analysis.

B. Software Functionality and Requirements

A number of requirements, both functional and general, drove the software design process. Some of the general requirements were that the software be clean, organized, and readable. If someone were to approach the code in the future with no background, they should be able to determine the design processes which guided the development and clearly see the architecture. In essence, this is the idea that the code should speak for itself. Another

requirement was that the software should be robust, well documented, and maintainable. If the hardware in the lab were to ever change, the code should be clearly documented so future programmers could quickly and easily make the necessary software changes. Additionally, the software should run smoothly and be able to withstand computer operating system updates. This leads to the next major guiding principle: it was desired that the software be cross platform. This way, the software does not restrict the lab to a specific operating system and the physical machine can be swapped out and run Linux, Windows, or Mac. Another restriction was the software should integrate with the previously chosen and pre-existing hardware components. These components include the LabJack ADC, PCB camera, and pressure and temperature sensors. The final general requirement was that the software provide a functional and intuitive graphical user interface (GUI).

The software also had several functional requirements and responsibilities. The software must read, process and display data from four pressure sensors on the supersonic nozzle, one pressure sensor on the tank, and one temperature sensor. Additionally, it must receive, process, and display a live video feed from the optical instrumentation camera. In addition to a "live view" mode, the software was to provide session recording functionality which would record both the live video and all six data inputs from the sensors, keep them synced together in time, and allow the information to be replayed again later. This meant the user interface must provide a means of starting and stopping the recording, selecting a directory and filename to save the data in, and re-opening that file and replaying it later. The final functional requirement was that the software should provide the ability to export the recorded sensor data in a user-friendly format such as comma separated values (csv) file. This would allow users to easily import the data into excel and perform any desired computations for further analysis.

C. Design Process and Development Stages

The development of the software consisted of four major stages, initial planning, feasibility testing, software development, and finalization. The initial planning stage consisted of outlining the software requirements and design criteria, researching the existing hardware, collecting datasheets, manuals, drivers for the hardware, researching and choosing the software language, libraries, and technologies, and curating the respective library documentation.

The second major stage of development, feasibility testing, was carried out via rapid prototype and concept development. The program was broken down into its major components and the new or unfamiliar concepts were highlighted as well as any components which would be "showstoppers" if they didn't work. These included the hardware, live sensor reading and data collection, basic GUI functionality, GUI window switching, live sensor data reporting, live video feed display, and simultaneous video and data capture, display, and saving. After the major hurdles were identified, many small programs were quickly developed to test and ensure the desired goal could be met. If the necessary functionality could not be produced during this testing stage, other solutions were sought and tested until one was found which would work.

The next major stage was the actual software development stage. To ensure the aforementioned requirements were met (such as clean, maintainable code) this stage began with software engineering. Before any final code was written, many hours were spent researching, planning, and discussing various design patterns and software architectures. Once an architecture was decided upon, diagramming began, and the software structure began to take form. Only after the structure was clearly captured and understood did the coding begin. The first step was to build the initial scaffolding for the software. This stage consisted of creating

base classes, interfaces, function stubs, etc. After the initial framework was in place, the core code, and live video and data feed capabilities was added. Next, the necessary data processing and handling was implemented, followed by sensor calibration capabilities to ensure measurement accuracy. After all the required functionality for a "live session" was implemented and functioning properly, development moved on to adding support for session recording. A number of different implementations were tried during this stage. The initial thought was to create a "replay session" view within the application itself which would read the raw sensor data file and video file and play them back together in the same manner as the "live session" view. However, after more time, thought, and discussion, this idea was abandoned in favor of a simple screen recording functionality. Screen recording would be easier to implement, reduce development time, and be more portable as students could take the video and replay it on any computer, anywhere, at any time instead of relying on the custom software package for replay. As a result, this is the method that was used in the end.

Once the software was complete, the finalization stage began. This stage was purely to ensure a polished and robust product. Exhaustive testing took place to ensure proper operation of all software and hardware components. Any necessary changes and final updates were implemented, and the finishing touches were put on. Finally, the documentation was updated to accurately reflect the software state and clearly communicate its design to future programmers.

D. Software Components

This project consists of both software and hardware components which must work together to create a final product. The most notable hardware components the software must integrate with are the LabJack UE9-Pro ADC (analog to digital converter for sensor data collection), and the ELP-USB13MAF-V75 PCB (printed circuit board) camera.

In addition to the hardware components, the software itself contains a number of components. These components can be placed in four overarching categories: core code, code, sensor and data collection related code, video related code, and graphical user interface code. The core code includes components such as file IO handlers, data converters and processors, configuration file readers and writers, and core program flow control. The sensor and data collection code includes interfaces and concrete classes for a live data reader (which communicates with the LabJack ADC), a data writer (which saves the data to a file on the hard disk drive), and a saved data reader (which reads the data from the disk). The video related code includes both interfaces and concrete implementations of a live video reader (which communicates with the PCB camera), a video writer/recorder, and a saved/recorded video reader. Lastly, the GUI contains several screens/windows and screen components. These are described in greater detail later, however the primary screens are the welcome window, the live session window, and some popup window dialogs used for setting adjustments and file selection.

E. Libraries, Modules, and Packages

Based on the requirements outlined earlier, several software technologies were selected. First, it was determined the Python would be the programming language used to write the custom software. One reason for this choice was Python's provisions for relatively fast prototyping and program development. Additionally, Python is an interpretive language which inherently makes it much more suitable for any type of cross-platform development, one of the desired software characteristics. Another major reason for this choice was because LabJack, the manufacturer of

the existing ADC, supplied libraries for custom software development in Python: namely, LabJackPython.

An open-source project called OpenCV was selected for the video capture and processing aspect of the project due to its widespread use and support. After a bit of research, DearPyGUI was selected as the framework to implement the graphical user interface. DearPyGUI is based off DearImGUI, which is a well-known immediate mode GUI library. DearPyGUI is sleek, supports multiple platforms, retains its appearance across all platforms, is designed around the immediate mode paradigm, and utilizes a systems GPU (graphical processing unit). In layman's terms, DearPyGUI is fast. A built-in csv module was used for writing and reading data files, and a module named ConfigParse was used for reading and writing the configuration and settings files.

F. Guiding Principles and Design Patterns

To keep the project clean, organized, and maintainable several guiding principles and design patterns were adhered to during the creation of the custom software package. The first major standard considered is Python's own style guide Python Enhancement Proposal version 8, more commonly referred to as PEP8. This style guide largely defines the code layout, formatting, and appearance, such as indentation, comments, whitespace rules, naming conventions, documentation strings (docstrings), function decorators, etc. as well as some general programming recommendations. Nearly all the guidelines set forth in the PEP8 standard are adhered to throughout this project. The naming conventions used in this project are summarized in **Table XI-1**. (Finer 2021).

***Table XI-1**: Naming conventions*

Type	Naming Convention	Examples
Function	Use a lowercase word or words. Separate words by underscores to improve readability.	function, my_function
Variable	Use a lowercase single letter, word, or words. Separate words with underscores to improve readability.	x, var, my_variable
Class	Start each word with a capital letter. Do not separate words with underscores. This style is called camel case.	Model, MyClass
Method	Use a lowercase word or words. Separate words with underscores to improve readability.	class_method, method
Constant	Use an uppercase single letter, word, or words. Separate words with underscores to improve readability.	CONSTANT, MY_CONSTANT
Module	Use a short, lowercase word or words. Separate words with underscores to improve readability.	module.py, my_module.py
Package	Use a short, lowercase word or words. Do not separate words with underscores.	package, mypackage

In addition to the PEP8 style guide, many other principles guided the design and structure of this program. Another primary goal was to keep the code neat, organized, and maintainable. To accomplish this, several tried-and-true software development principles, design patterns, and

programming paradigms were used to guide the software architecture. These include principles such as OOP, SOLID, YAGNI, DRY, CQRS, and the Clean Code Architecture.

OOP stands for Object Oriented Programming, which is the overarching programming paradigm used in this project ("Object-Oriented Programming" 2022). A major design principle that comes right alongside OOP is SOLID. SOLID is an acronym for a set of five design principles. The first is the Single Responsibility Principle, every class or function should have a single responsibility. Next is the Open-Closed Principle which states, "Software entities should be open for extension, but closed for modification". Third, is the Liskov Substitution Principle, functions that use base classes must be able to use objects of derived classes without knowing it. The fourth principle is the Interface Segregation Principle which states, "Many client-specific interfaces are better than one general-purpose interface." The final design principle is the Dependency Inversion Principle, which says code should "Depend upon abstractions, [not] concretions," ("SOLID " 2022). These design principles greatly enhance code organization, clarity, and ease maintenance. Further discussion regarding these principles and their implementation in the software for this project is provided in the Software Architecture section of this paper.

YAGNI is an acronym for, "You Aren't Gonna Need It". This is a mantra commonly used in agile software development teams which essentially states a programmer should not waste time implementing things before they are deemed necessary (Fowler, Martin 2015) ("You Aren't Gonna Need It" 2022). DRY is another widely used software development principle which stands for "Don't Repeat Yourself". DRY aims to reduce repetition, duplication, and cross dependencies among software by requiring "Every piece of knowledge must have a single, unambiguous, authoritative representation within a system," ("Don't Repeat Yourself" 2022). DRY suggests using abstractions, methods, subroutines, etc. to accomplish this. This principle is vitally important, as breaking it wastes time, leads to "spaghetti code", and makes debugging and maintenance a nightmare. Another design principle this project borrowed from is CQRS (Command-Query Response Separation) (Fowler, Martin 2011). At the core of this principle is separation of concerns. Every function operating on a database should be a command that performs an action or returns data, but not both. In layman's terms, "asking a question should not change the answer," ("Command-query separation" 2022) (Meyer, Bertrand 2012). This principle is largely what led to the development of separate reader and writer interfaces and modules within the custom software for this project. Another guiding principle to ensure a clean and maintainable architecture was avoiding global variables and global state dependence. Whenever possible, the necessary variables were passed into a function or class to prevent creating a mess of dependencies with the entire program relying on a single variable shared across multiple modules.

The final major design guideline was Clean Code Architecture system by Robert C. Martin (Martin, Robert C. 2012). This architecture outlines major software layers/boundaries to help create clean, readable, testable, and maintainable code. Each layer can communicate with the layer immediately above or below it, but none of the other layers. This creates a beautifully independent system where any layer and library dependency can be swapped out for another without breaking the whole system and requiring an entire software rewrite. For example, should the physical hardware such as the ADC or camera change in this project, only a single module would need to be re-written. Even though the live sensor data is processed and displayed in the GUI, neither the processing layer, nor the GUI layer would need to be touched as they are

written to be completely independent of the underlying system. Further details of the application of this architecture are provided in the Software Architecture section of this paper.

G. Software Architecture

At the most basic level, this program can be divided into three main levels a user level, a software level, and hardware level. This is illustrated in **Table XI-1**. All three of these levels contain code, however they are separate and have distinct responsibilities. The user interacts with the program at the user level by clicking buttons, dragging sliders, etc. on the graphical user interface. The software level then connects these actions with the underlying hardware level. The hardware level is then responsible for querying the physical devices in the laboratory and making any necessary changes such as getting a new video frame, updating the camera focus, or calibrating a sensor. **Figure XI-1: Basic Program Hierarchy** provides the most basic view of abstraction implemented in the software. Each level may depend on, or use, the levels adjacent to it, but no further. For example, the GUI should not directly depend on a specific hardware device being used. If a new ADC is needed, none of the GUI code should have to change.

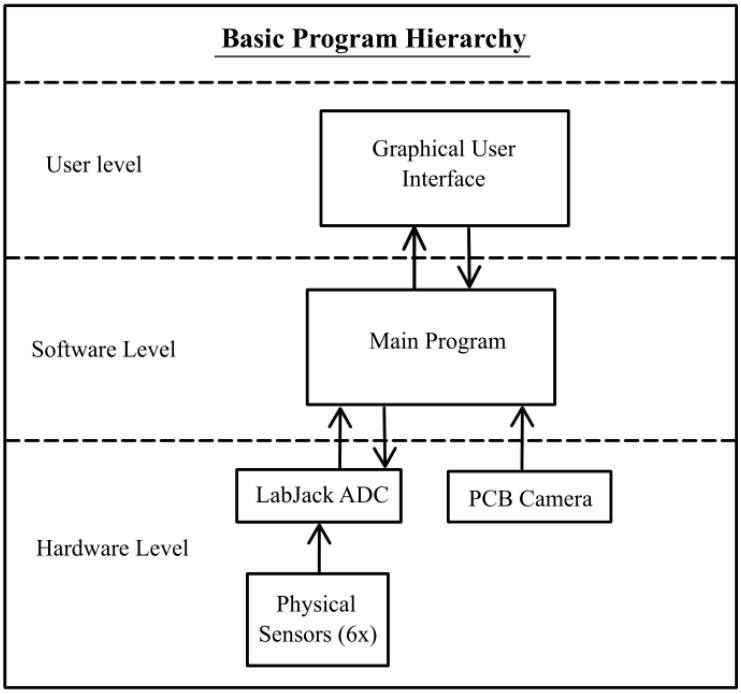

***Figure XI-1**: Basic Program Hierarchy*

The program can be further broken down into smaller layers of abstraction. A much more detailed diagram of the software's abstraction hierarchy may be seen in **Figure XI-2**.

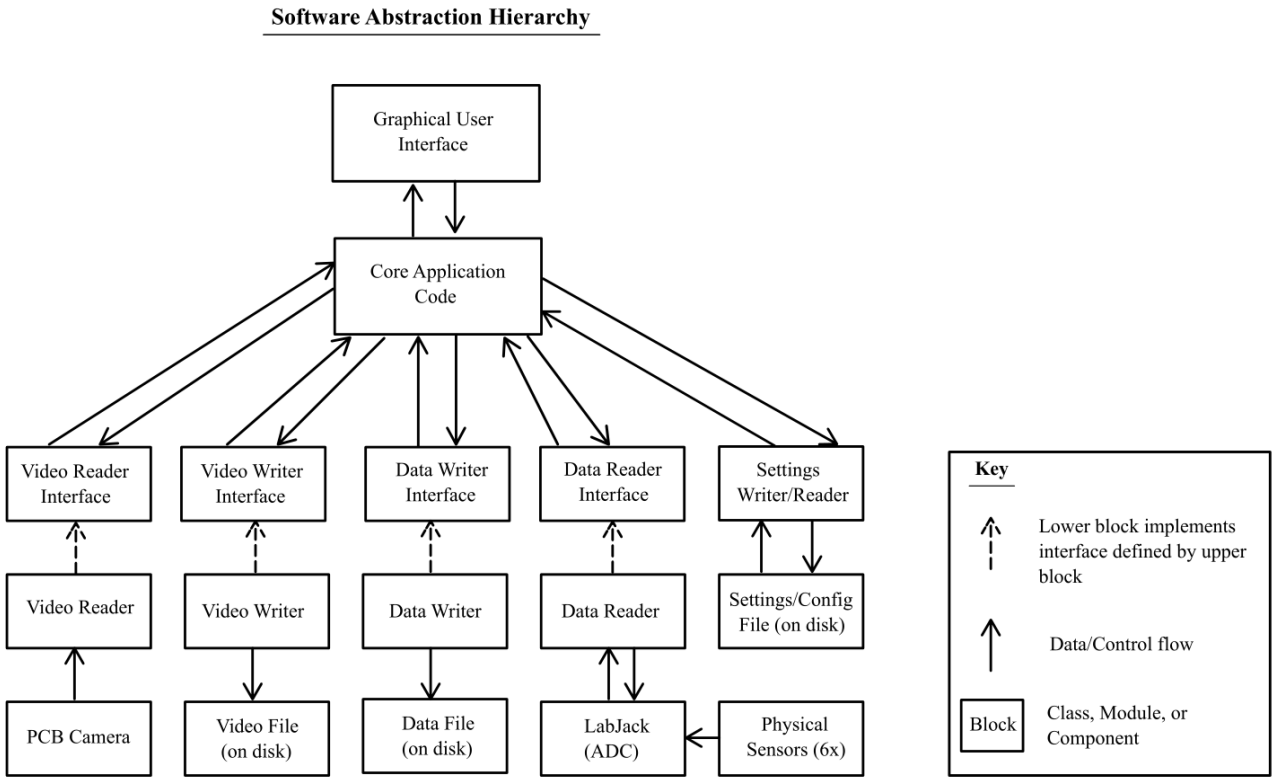

Figure XI-2: *Software Abstraction Hierarchy*

Figure XI-2 shows five overarching layers. The GUI is still at the top, followed by the core application code. After that, however, a new layer is included. This layer is the interface layer. An interface is a portion of code which outlines the requirements another section of code must meet (or implement). This allows multiple concrete implementations of a single interface. For example, a section of code at the interface level may define what a video frame should contain, and then there can be two different implementations of that interface at the concrete level which both provide the specified video frame, but one may obtain it from the camera, while the other may obtain it from a file saved on the disk. Due to the specific nature of this program and the aforementioned CQRS principle, this program separates those two actions, however the example remains valid as an illustration. The level shown below the interface level is the concrete implementation level. The final level on the bottom is the hardware/peripherals level, it contains data or physical devices which the concrete functions/classes interact with.

As mentioned previously, the Clean Code Architecture played a major role in guiding the design of this software. A clear demonstration of its use in this software's architecture can be seen in **Figure XI-3**.

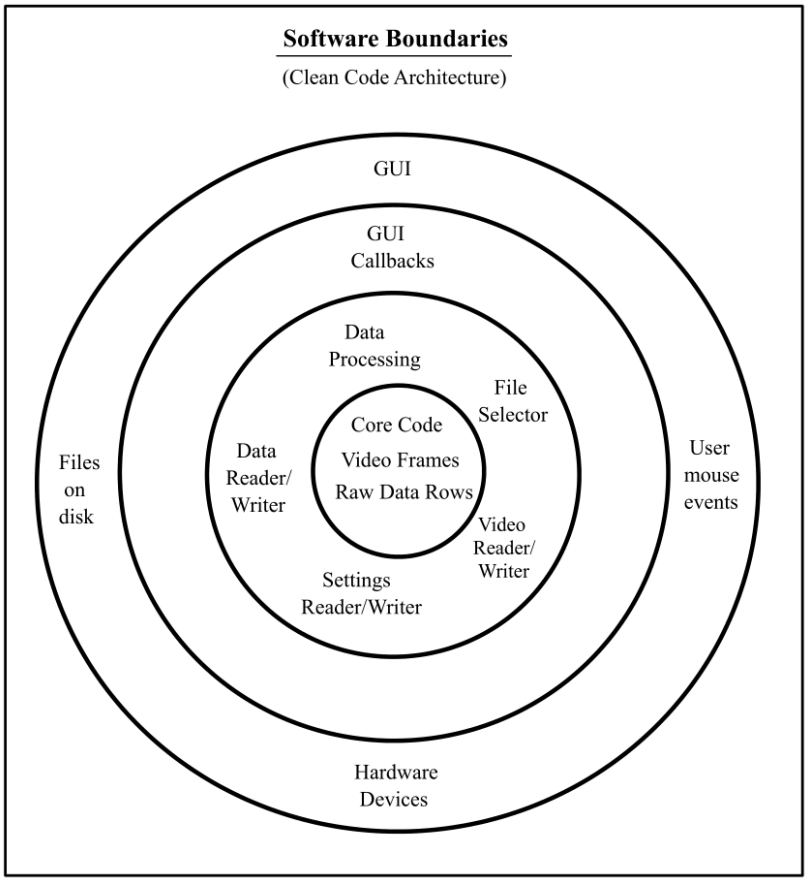

Figure XI-3: *Software Boundaries Diagram*

Figure XI-3 outlines the boundaries between the various software layers and shows where the major components lie within the system. At the center of the image are entities and core code. These are things such as the video frames, and raw data rows which contain the sensor data. The next ring contains components which rely upon entities in the center and communicate with code in the next ring out. Code within this boundary layer includes code which reads, writes, and processes video frames, sensor data, and other files. The third ring acts as the primary communication channel between the outermost ring and the majority of the code. Whenever a user clicks a button on the GUI, the callback layer will call a function in the second ring to perform the desired action. The outermost ring contains the components at the outermost layer of the system such as files located on the computer's hard drive, hardware devices, the GUI, and the user's interaction with it. Separating the code in this manner has many benefits, but the most notable are improved organization, readability, independence, and maintainability.

H. Graphical User Interface Design

The GUI plays a significant role in this project. It is the primary means by which a user can interact with the system, collect, visualize, and process the lab data. As a result, careful thought and planning has been put into this aspect of the software design to ensure a functional and intuitive interface. Two primary screens and a few additional windows/dialogs have been identified as the primary constituents of the GUI. These are described in the following section.

Primary Screens and Windows

The first primary window is the "Welcome Window". A wireframe model of this screen outlining its primary functional components is provided in **Figure XI-4**. The second primary screen is the "Live Session Window". This screen is used anytime a user desires to monitor or record live data coming from the PCB camera and physical sensors. See **Figure XI-5** for a wireframe of this screen's main components.

In addition to the primary windows, there are also a few popup windows and helper dialogs. One of these is the "File Selection Dialog". This dialog is displayed on two occasions with a slight variation between the two. The first is whenever the user needs to select a file to open, and the second is whenever the user needs to specify a location to save a file. In the first case, only the "Open" button will be displayed, while in the second case, only the "Save" button will be visible. A basic concept for this window is provided in **Figure XI-6**.

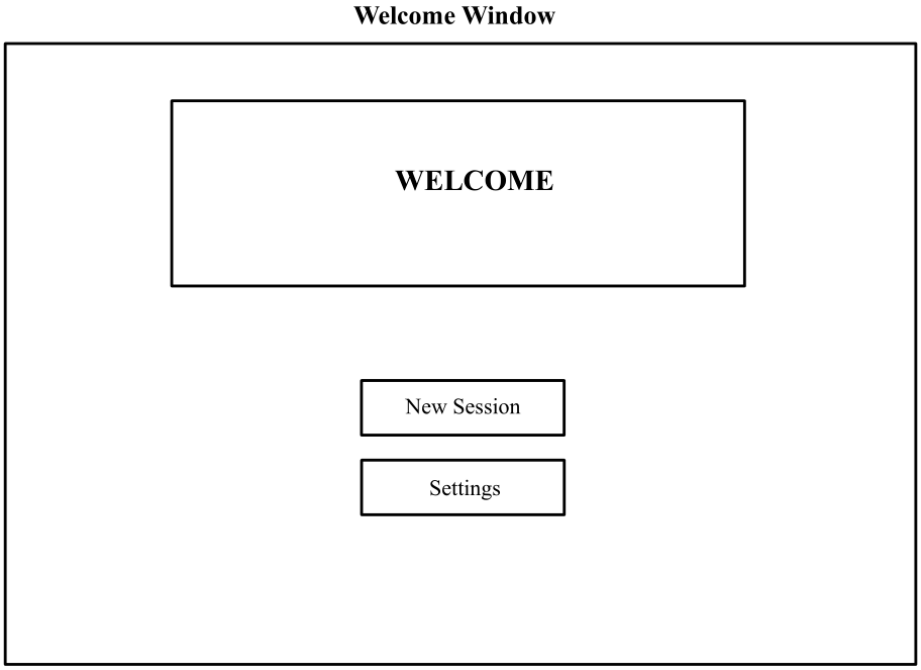

***Figure XI-4**: Welcome Window*

Live Session Window

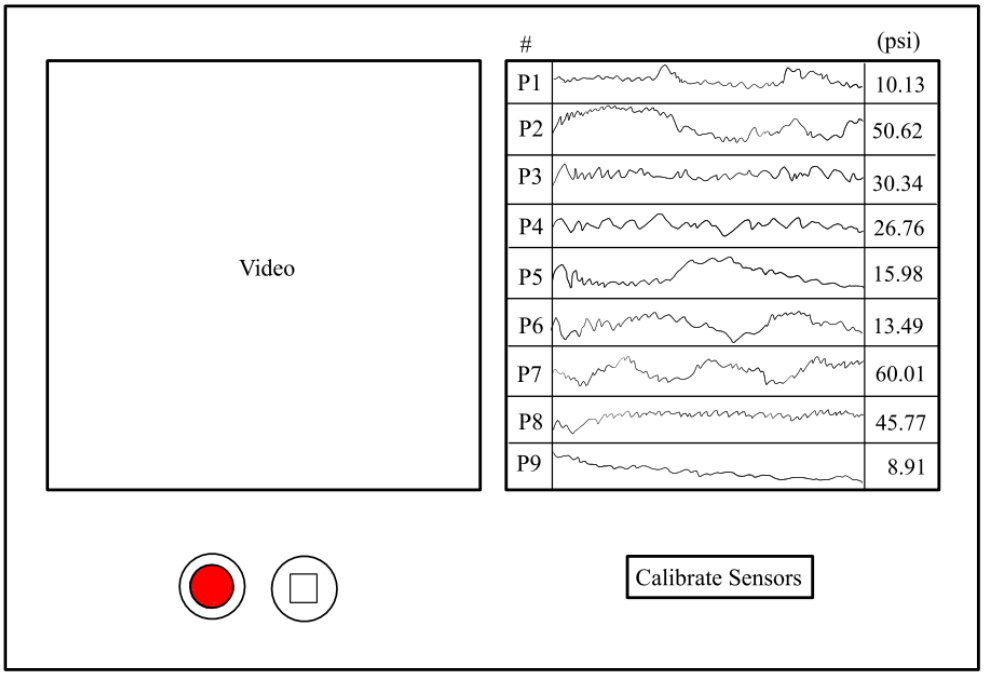

***Figure XI-5**: Live Session Window*

Popup: File Selection Dialog

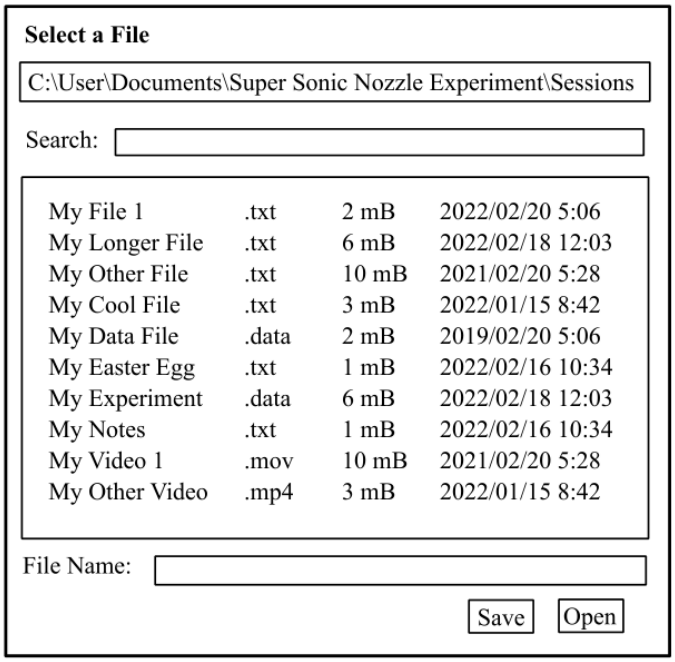

***Figure XI-6**: File Selection Dialog*

Screen Progression and UI Flow

The navigational flow between the primary screens and dialogs is captured in **Figure XI-7**. Upon opening the program, the user is greeted with the Welcome Window and presented with two primary options: new session or settings. Upon selecting a new session, the user is directed to the Live Session Window which presents live data from the optical instrumentation camera and the systems six physical sensors. This screen also provides options to start and stop recording. If the user chooses to record the live session, they will be presented with a new popup window which asks them to select the director and filename in which the data will be stored. Once the location and name are specified, the user may click "Save" which directs them back to the Live Session Window, except the "Start Recording" option has been updated to a "Stop Recording" option. Once the lab experiment is done and the user has collected all necessary data points, they may click "Stop Recording" which directs them back to the initial Live Session Window with the option to start a new recording. Once the user is done, they may return to the Welcome Window again by clicking the "Home/Back" button, or they may simple close the application.

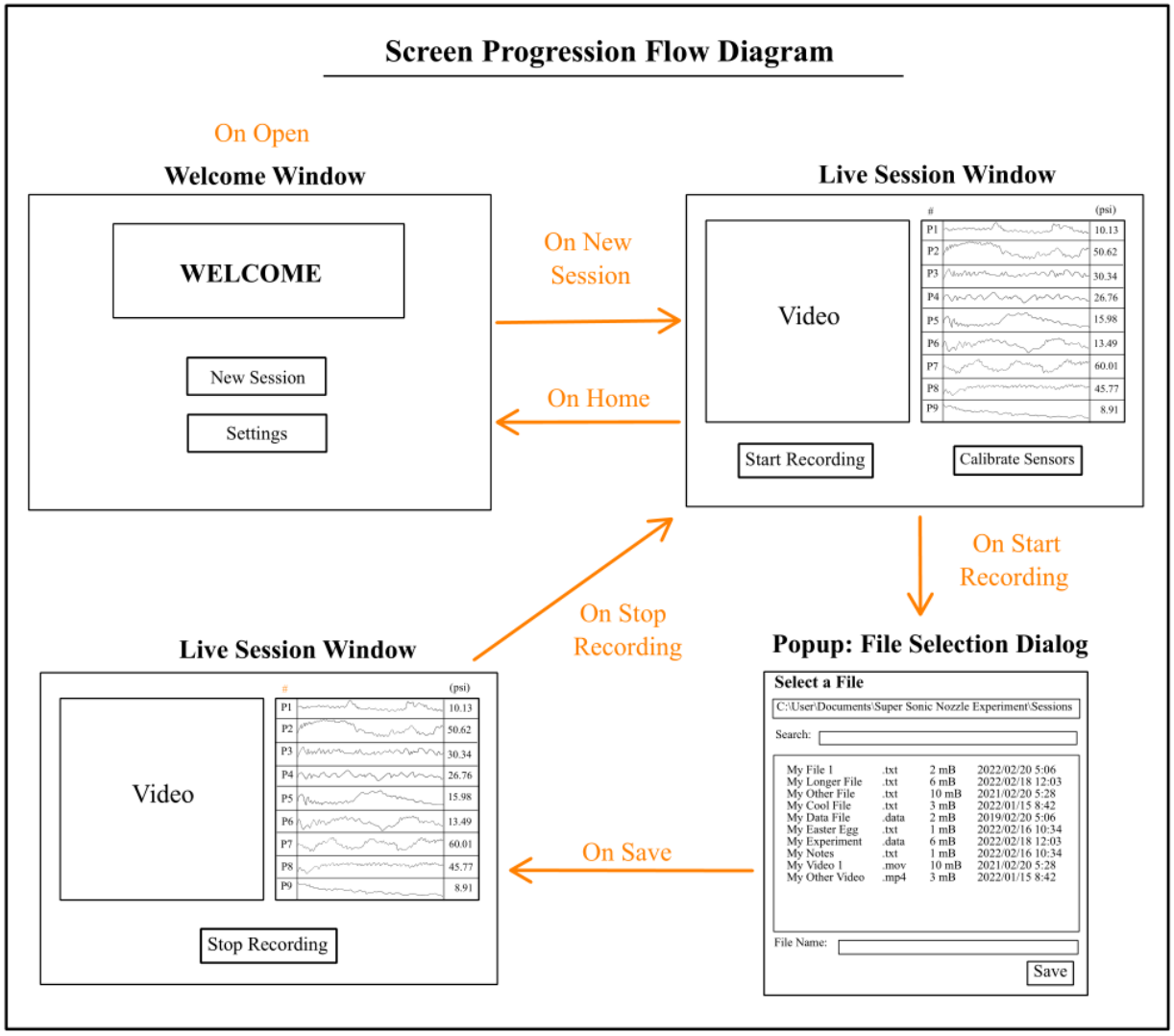

***Figure XI-7**: Screen Progression Flow Diagram*

I. Installation Guide

For a complete installation guide, see the "quick start/installation" section of the "readme" file available on the project's GitHub page (Nelson 2022).

J. Maintenance Guide

For a complete maintenance guide, see the "maintenance" section of the "readme" file available on the project's GitHub page (Nelson 2022).

XII. Educational Materials

All of the work discussed previously in this paper is important to making an experiment that functions properly and safely, in a way that students can easily access and use. However, none of this matters if the students do not know how to conduct the experiment or interpret its results. For this purpose, educational materials needed to be generated in order to aid in this process.

A. Laboratory Handout

For a student to complete a laboratory experiment as a part of the Fluid Mechanics Laboratory, a laboratory handout is required. Such a handout includes an explanation of the apparatus involved in the experiment, a treatise on the theory involved in the experiment, and clear expectations as to what types of data analysis and conclusions they are supposed to draw from the experiment. A laboratory handout must be both sufficiently detailed for students to effectively complete the lab, but also sufficiently vague to allow students to discover and apply the knowledge they have coming into the experiment.

A laboratory handout was carefully created for Dr. Thomsen for the purposes stated above. A copy of this handout is included in **Appendix D: Supersonic Nozzle Experiment Laboratory Handout**. The handout carefully describes how to calibrate the pressure sensors, fill the tank, stop the filling process, run the air through the nozzle, and drain the nozzle afterwards. It also describes the theory of compressible flow as applied to converging-diverging nozzles in great detail, with additional information included about oblique shockwaves that were not covered in Fluid Mechanics class. Finally, explicit instructions on what graphs to create and what questions should be answered using them, were written, and are included in the handout. In the future, it would be beneficial to add a section about how to operate the software as well.

XIII. Manufacturing and Testing

On this project, our team did a small amount of manufacturing, but overall, it did not need to be precise, and each step of manufacturing is included in previous sections throughout this paper. As described in the **Installation and Assembly** section, tables and stands created to hold the tank and optics assembly were manufactured using wood, wood screws, and wood. Additionally, the **Optical Instrumentation** section describes how the mounts were 3D-printed and manufactured out of aluminum beams. Finally, the construction of a baseboard and plexiglass shield for the data-acquisition system are described in the **Pressure and Temperature Instrumentation** section.

As for testing, we were able to test that the device functioned without breaking, and that a small shockwave could be observed, when testing the system at a pressure of 120 psi. However, since the booster pump did not end up being functional this year, high-pressure testing at 600 psi was not possible. A complete test of the entire system together will need to be completed in the

future once the software package is complete, and so has not been completed yet because of that. In addition to testing the entire system, each project section was tested as much as possible on its own in an isolated manner. These tests and their results are included in the **Installation and Assembly**, **Optical Instrumentation**, and **Pressure and Temperature Instrumentation** sections of this paper.

While the software development aspect of this project did not adhere to the Test-Driven Development (TDD) design process in its fullest sense, the overarching concept was very influential in the design process. Testing was performed at every step throughout the development process. Though no explicit test code was written, each function, module, and component was manually tested after it was written to ensure proper operation. Software testing was not limited to this, however, as tests were also conducted to ensure proper sensor calibration, accurate temperature and pressure readings and unit conversions, valid file saving, and correct and accurate data acquisition and exportation.

XIV. Project Evaluation

To date, the assembly and installation of the device is fully completed in terms of what was set out to be accomplished at the beginning of the academic calendar and more. Several objectives were added to the scope that were not originally part of the division that were also completed, while others were taken off the check list. The design meets all of the design criteria and constraints. The device stand and optics stand were created to allow for the tank to be drained, provide a platform for the tank to be operated and viewed at a comfortable eye level, as well as create a space for instrumentation to be attached and stored within. The stand(s) met all three of these objectives which they initially sought to accomplish.

Both the device stand and optical stand meet practical, economical, and safety constraints in that they were relatively cheap to build in comparison to anything that could be purchased on the market. They were overbuilt according to hand calculations and finite element analysis to provide for a space environment for future users, and economic in their design. Rather than choosing a design that might be difficult for a beginner in woodwork, these stands were simple to construct and would be simple to deconstruct in the chance that they would ever need to be moved.

While the assembly and installation of this device did not have a direct effect on the environmental, societal, and global realms of the school of engineering nor this Walla Walla University campus, one could argue that by the construction of this device will enable future students for generations. The impact of this project may not be seen or felt immediately, but the societal and global impacts it could have on the world because of the knowledge that it will share with incoming fluids students is immeasurable.

As mentioned in Codes and Standards, a handful of regulations and constraints were considered for the assembly and installation of this device. From American Wood Council standards for the device and optics stand (AWC EWC 2018) to university guidelines regarding student safety and wellbeing (McVay, John 2020) and Washington Statue guidelines for in-school laboratory experiments (Washington State Legislature). Beyond these standards, section 8 of the ASME BPVC guidelines were also considered during the installation of the device. Because the tank deals with relatively high pressures, it was important to include a pressure relief valve and include warning tags on the device itself as well as in the student handout that each user will be required to read through before beginning the experiment. The codes and standards that were followed during the completion of this project ultimately helped guide in the process of

decision making and considerations regarding health and wellbeing of future students who will be conducting this laboratory experiment.

The optical instrumentation meets the standards required. The mounting system needed to be adjustable, and the image needed to be clear and understandable to students. We have achieved both of those criterial. Though there were no official codes to be met, we made this part of the project as safe for students as possible. Lasers were avoided, not sharp edges were left, and the mounting is tight enough to keep from being adjusted accidently. 3D printing our parts, working with Professor Sterling to get railing and finding inexpensive lenses also made this part of the project in expensive.

The pressure and temperature instrumentation portion of this project was fully completed, and all objectives were met. Holes were drilled in the nozzle normal to the surface of the converging-diverging nozzle at the proper cross-sectional areas within appropriate bounds. Additionally, the pressure sensors ordered were selected and tested at the pressure ranges expected in the nozzle at each point and were found to be perfectly suited to the task. There were no relevant codes and standards that were directly used in the assembly of the pressure and temperature instrumentation on the tank. However, all tubing, fittings, and sensors that were purchased were rated for the pressure ranges and temperature ranges expected from the experiment, meaning that the manufacturer made sure they were within the standards necessary. This, in addition to careful installation of these components, ensured that nobody would be hurt, and nothing would break in the operation of the data-acquisition inherent in the project. Because everything is functional and will soon be able to be operated with ease and safety, all practical and safety constraints have been met for this part of the project. Additionally, all components ordered were carefully researched and considered, keeping the costs as low as possible for this portion of the project. Specific parts were found at the cheapest source possible, resulting in much lower expenditures than expected, satisfying economic constraints for this portion of the project as well.

The custom software package developed as part of this project met all the respective design criteria and constraints. At a high level, it was desired that the software for this project be cross platform supporting both Windows and Linux operating systems to increase flexibility and prevent it from being tied to specific systems. This was accomplished by using Python as the primary development language and using only platform independent packages. Furthermore, due to the choice of the underlying libraries, the UI maintains a uniform appearance independent of what operating system the software is run on.

The software package also met all the practical and functional requirements. The software provides a functional and intuitive GUI for students to use without the need to read any complex user manual. The software successfully displays the video feed from the optical instrumentation/schlieren imaging camera of the nozzle so students can visually see the shockwave and supersonic flow that occurs within the nozzle in real-time. Additionally, the software correctly reports measurements from the various temperature and pressure sensors located throughout the system. It continuously polls all six instrumentation sensors, performs all necessary unit conversions, applies all calibration correction factors, and plots the data in real-time all while simultaneously saving the data. The software package also allows users to start and stop recording live sessions which can then be saved in a portable video format and transferred to any computer for future reference or replay. Finally, the software also met the data exportation objectives. It accomplished this by providing the ability to export all recorded

sensor data to a comma-separated-value (csv) file which is a user-friendly format which can easily be imported into Microsoft Excel or similar processing software for further analysis.

The code written for the custom software package also had a number of objectives and constraints of its own which were also met. The code successfully integrates with all the pre-existing hardware components including the PCB camera, the LabJack ADC, and its associated instrumentation and amplifiers. Another major constraint placed upon the code was that it should be clean, organized, and readable. A number of codes and standards and programing paradigms played an important role in ensuring the code met this constraint. One of the most notable in Robert C. Martin's Clean Code Architecture. This programming standard really helped ensure a clean and maintainable design. Python's PEP8 set of standards also played a critical role in creating readable and familiar code by following the recommended naming conventions and comment, docstring, and decorator formats. The Object-Oriented programming paradigm along with the five standards outlined by SOLID proved vitally important in keeping the project organized. Right alongside these, the principles set forth by the DRY and CQRS programming standards were also found to be very instrumental in ensuring the design met the maintenance and flexibility constraints set forth at the beginning of this project.
Another significant objective of the code was to create a robust, flexible, and sustainable software application which could be easily maintained throughout the years to come. This was accomplished via multiple avenues. As described previously, the whole software architecture was designed with this in mind, and the code was carefully constructed to decouple the low-level hardware from the GUI. The "separation of concerns" principle was very influential at every step of the way and resulted in a product that allows the low-level hardware, such as the ADC or the PCB camera, to be switched out without the need to re-write any of the front-facing GUI code. In addition to being designed with flexibility in mind, the code was also well documented. This greatly enhances the sustainability of the project by easing maintenance for any future work should it ever be deemed necessary. To accomplish this, the code was well documented with comments and docstrings throughout. Furthermore, a final "readme" file was created which clearly detailed all the important aspects of the project including a "quick start guide" and a "maintenance guide". This documentation is all available on the software project's GitHub page (Nelson 2022).

As for the educational preparation section of the project, a laboratory handout was created, as expected, but a video and sample key were not created, as the experiment cannot yet be fully run. The handout was approved by Dr. Thomsen, however, and as a result should meet all of the educational standards set by the university and the accreditation requirements being met by the Fluid Mechanics Laboratory class.

XV. Impacts

The software developed for this project may seem inconsequential in the grand scheme of things, however its impact may be much farther reaching than anyone will know. The custom software package enhances the learning process by allowing students to study compressible flow by conducting the laboratory experiment, monitoring it in real-time, collating the results, and exporting them for further study. This enables students to gain the experience, understanding, and insight necessary to prepare them for a successful career which may benefit society for generations.

As a whole, our project has the potential to have wide-reaching impacts on future students, Walla Walla University, and the world. Most obviously, this experiment will allow

future students to gain a better understanding of compressible flow, strengthening their education and making them better engineers. Though it may seem trivial to some, this could actually have widespread effects. First, engineering students graduating with a stronger understanding of compressible flow and data analysis in general will likely go on to be more effective engineers in their careers. For example, some of these engineers will likely contribute to the design and analysis of propulsion systems, and they will be more equipped to design such systems in a way that is more sustainable, reduces noise, and minimizes chemical pollution. This, in turn, would cause improvement in the environment and global society as a whole.

Additionally, this experiment will also improve the quality of education at Walla Walla University, serving as an example to visitors, potential students, and even potential employers of those students the continued excellence of this university's educational programs. For example, the schlieren imaging system has already been used in a guest lecture at a local high school, to introduce them to engineering in a visually stunning manner. This could ultimately have the effect of increasing enrollment in the engineering program and the success of its graduates.

Ultimately, many of these impacts may seem farfetched. However, there is no telling what the ultimate impacts of a project may be, and the aforementioned impacts are all possible repercussions of our project. After thinking about the project at length, there do not appear to be any significant cultural, political, or health-related impacts.

XVI. Future Work

As it stands, the installation and construction of the project is fully complete. However, the device is not fully functioning at the moment. Unfortunately, the booster pump purchased from SC Hydraulic has experienced issues with boosting the 120-psi shop air up to 600 psi for the purposes of the experiment. While a considerable amount of work and consultation has put into troubleshooting the issue, a solution is still yet to be found for the booster pump. For this reason, it was decided to return the pump to the manufacturer for inspection and repair. Once the pump is returned this summer, Technical Support Services will be asked to reinstall the pump. If Dr. Thomsen finds it necessary to continue the project for one more year to tie up loose ends with hardware testing, safety risk mitigation, and lab handout creation, a single senior could be asked to help complete the project as their senior capstone project. If the project is found to be close enough to completion, TSS and Dr. Thomsen will tie up these loose ends and the experiment will be ready for use next Winter.

Upon hardware testing at high pressures, issues with the current resin nozzle might be revealed (cracking or blowout), in which case a second nozzle, made with a new material, will need to be incorporated for the device to be used at full capacity. Additionally, upon testing at high pressures, the project sponsor might find it beneficial to the safety of operators to incorporate a plexiglass viewing screen. The idea of a viewing screen was discussed several times during project assembly, however other additions to the scope of construction and assembly division of the project took precedence over the possibility of a screen up until the completion of the academic year.

The optical instrumentation is complete and functional for this project. Future work would be to improve it. First, tapping plastic is not ideal because the threads strip easily. It is much better to tap into mettle. A task could be to change the plastic parts of this project to steel or aluminum.

The pressure and temperature instrumentation portion of the project is mostly complete, and there is very little future work to be done on it. However, it does need to be wired up to the

analog-to-digital converter, and then tested using the software interface that has been developed. This is something that, while simple, must still be completed in the future.

While the current software package meets all the project requirements and provides all the necessary functionality there is still opportunities for future improvement. One weakness is the inability to dynamical rescale the UI window and all the GUI elements within the window. Currently all UI elements are sized for display on a 1920x1080 pixel screen. As it stands, the viewing window can be resized, however the size and resolution of the live video feed is not resized. Another area that could be improved is the installation process. Currently installation requires a number of steps which may be overwhelming for new users unfamiliar with programming. The ease of installation was not a primary focus during the development of this project because under the intended use the program will only need to be installed once on a lab computer. However, should the physical computer ever need to be swapped out or updated, it would be beneficial to have a pre-packaged executable installer. Ideally this installer should carry all necessary libraries and dependencies and perform all the setup and installation steps required to get the program up and running with just a few clicks. This could probably be best accomplished using the PyInstaller package. A final area for future work in the software is better operating system cross-compatibility support. Further testing could be performed to ensure the software runs smoothly on both Windows and Linux. More specifically, program execution could be tested on multiple distributions of Linux (e.g., Solaris, Ubuntu, Arch, etc.) and multiple versions of Windows (e.g., Windows 7, 10, 11) as well as various CPU-bit architectures (i.e., 64-bit or 32-bit). Additionally, further research could be conducted to decrease the program's startup time on Linux. While operating system cross compatibility was one of the objectives for this software, it was not an essential requirement as the primary goal was to get the software up and running on a single lab machine. The desire for cross compatibility arose as a superfluous goal to allow for even greater flexibility and sustainability should a different host operating system ever be desired. While there is opportunity for future work, the current software meets or exceeds all the criteria and objectives set forth at the beginning of the project.

The educational materials for this project also have a few tasks that have yet to be completed. First a laboratory report key must be written, so that whoever grades the laboratory reports can have a guide as to how to grade them. Then, a video must be made describing the lab and showing the students how to operate and conduct it.

XVII. References

American Wood Council. 2018. *Manual for Engineered Wood Construction.* Leesburg, VA: American Wood Council.

ASME PTC. 1974. "Temperature Measurement." *American Society of Mechanical Engineers Performance Test Codes* 19.3-1974 (R2004). codes-standards/ptc-19-3-temperature-measurement?productKey=C0003P:C0003P.

ASME. 1981. "Wood Screws (Inch Series)." *American Society of Mechanical Engineers* B18.6.1. https://standards.globalspec.com/std/519727/ASME%20B18.6.1.

ASME BPVC. "Rules for Construction of Pressure Vessels." *American Society of Mechanical Engineers Boilers and Pressure Vessel Codes* VIII.1-2021 (R2021). https://www.asme.org/codes-standards/find-codes-standards/bpvc-viii-1-bpvc-section-viii-rules-construction-pressure-vessels-division-1/2021/print-book.

ASME PTC. 2008. "Data Acquisition Systems." *American Society of Mechanical Engineers Performance Test Codes* 19.22-2007 (R2017). https://www.asme.org/codes-standards/find-codes-standards/ptc-19-22-data-acquisition-systems.

ASME PTC. 2010. "Pressure Measurement." *American Society of Mechanical Engineers Performance Test Codes* 19.2-2010 (R2020). https://www.asme.org/codes-standards/find-codes-standards/ptc-19-2-pressure-measurement

Bailey, Parker and Jonathen Stacy. 2020. "Supersonic Flow Device." Senior Project Paper, Walla Walla University.

Barbour, Ethan, Ronald Hanson, Chris Morris, and Matei Radeulescu. 2012. "A Pulsed Detonation Tube with a Converging-Diverging Nozzle Operating at Different Pressure Ratios." *American Institute of Aeronautics and Astronautics* 2005-1307: *43rd AIAA Aerospace Sciences Meeting and Exhibit*. https://doi.org/10.2514/6.2005-1307.

Barbour, Ethan, Zachary Owens, C. Morris, and Ronald Hanson. 2004. "The Impact of a Converging-Diverging Nozzle on PDE Performance and its Associated Flowfield." *American Institute of Aeronautics and Astronautics* 2005-1307: *42nd AIAA Aerospace Sciences Meeting and Exhibit*. https://doi.org/10.2514/6.2004-867.

Bose, T.K. 1967. "Effect of Heat Transfer in a Converging-Diverging Nozzle." *Journal of Spacecraft and Rockets* 4 (3). https://doi.org/10.2514/3.28873.

Chen, Shuxing. 2009. "Compressible Flow and Transonic Shock in a Diverging Nozzle." *Commun. Math. Phys* 289: 75-106. https://doi.org/10.2514/1.A34616.

"Command–Query Separation." Wikipedia. Wikimedia Foundation, January 19, 2022. https://en.wikipedia.org/wiki/Command%E2%80%93query_separation.

Davidhazy, Andrew. "Introduction to Shadowgraph and Schlieren Imaging." 2006. *Rochester Institute of Technology*, 1–59.

"Don't Repeat Yourself." Wikipedia. Wikimedia Foundation, February 8, 2022. https://en.wikipedia.org/wiki/Don%27t_repeat_yourself.

EF Cross School of Engineering. 2017. *Engineering Lab Report Standard*. Walla Walla University.

Finer, Jasmine. "How to Write Beautiful Python Code with PEP 8." Real Python. Real Python, March 6, 2021. https://realpython.com/python-pep8/.

Fowler, Martin. "Bliki: CQRS." martinfowler.com, July 14, 2011. https://martinfowler.com/bliki/CQRS.html.

Fowler, Martin. “Bliki: Yagni.” martinfowler.com, May 26, 2015. https://martinfowler.com/bliki/Yagni.html.

Hibbler, R.C. 2017. *Mechanics of Materials*. Hoboken, NJ: Pearson.

How To: Build Your Own Schlieren Setup, YouTube. Accessed November 15, 2021. https://www.youtube.com/watch?v=IZ0bYi9UFv8.

Huang, He-Ji, Wen-Xia Pan, and Cheng-Kang Wu. 2018. “Aerodynamic Dispersion of Anode Arc Attachment Through a Converging-Diverging Nozzle.” *IEEE Transactions on Plasma Science* 47 (1): 847-852. https://doi.org/10.1109/TPS.2018.2880246.

Jee, Craig and J. Etele. 2020. Optimization of a Supersonic Rocket-Based Combined Cycle Inlet Using Differential Evolution.” *Journal of Spacecraft and Rockets* 57 (3): 496-509. https://doi.org/10.2514/1.A34616.

Keller, Robert. *The 1-Hour Workbench / Outfeed Table // Woodworking DIY*. 2019. YouTube. Accessed November 15, 2021. https://www.youtube.com/watch?v=PMJ4Lob5Q4I

Liu, Yi. 2007. “The Use of Miniature Supersonic Nozzles for Microparticle Acceleration: A Numerical Study.” *IEEE Transactions on Biomedical Engineering* 54 (10): 1814-1821. https://doi.org/10.1109/TBME.2007.892919.

McVay, John. 2020. *John McVay to Walla Walla University Faculty, Administration, and Staff.* Letter. From Walla Walla University. https://www.wallawalla.edu/fileadmin/user_upload/Risk_and_Safety/Forms-Other/President_s_Safety_Letter.pdf.

Mariani, R., B. Zang, H.D. Lim, U.S. Vevek, T.H. New, and Y.D. Cui. 2019. “A Comparative Study on the Use of Calibrated and Rainbow Schlieren Techniques in Axisymmetric Supersonic Jets.” *Flow Measurement and Instrumentation* 66: 218–28. https://doi.org/10.1016/j.flowmeasinst.2019.01.007

Mazumdar, Amrita. “Principles and Techniques of Schlieren Imaging Systems.” June 18, 2013. *Department of Computer Science,* 1–16. https://doi.org/https://doi.org/10.7916/D8TX3PWV

Martin, Robert C. “The Clean Code Blog.” Clean Coder Blog. Clean Code Blog, August 13, 2012. https://blog.cleancoder.com/uncle-bob/2012/08/13/the-clean-architecture.html.

Meyer, Bertrand. “Eiffel: a Language for Software Engineering.” Eiffel Laser Foundation. Laser, 2012. http://laser.inf.ethz.ch/2012/slides/Meyer/eiffel_laser_2012.pdf.

Nelson, Caleb. “Supersonic Nozzle Control Center.” GitHub, 2022. https://github.com/Dizzerin/Supersonic-Nozzle-Control-Center.

“Object-Oriented Programming.” Wikipedia. Wikimedia Foundation, February 1, 2022. https://en.wikipedia.org/wiki/Object-oriented_programming.

OSHA. “Occupational Safety and Health Standards.” *Occupational Safety and Health Administration* 1910.95 – Occupational noise exposure. (R2008). https://www.osha.gov/laws-regs/regulations/standardnumber/1910/1910.95.

“Solid.” Wikipedia. Wikimedia Foundation, February 1, 2022. https://en.wikipedia.org/wiki/SOLID.

Thomsen, Doug. 2021. *Engineering364_Syllabus_W21*. Fluids Laboratory Handout, Walla Walla University.

“Understanding Collimation to Determine Optical Lens Focal Length.” Edmund Optics Worldwide. Accessed November 15, 2021. https://www.edmundoptics.com/knowledge-center/video/tutorials/understanding-collimation-to-determine-optical-lens-focal-length/.

Washington State Legislature. 2021. “Working Space Around Electrical Equipment.”

Washington State Legislature WAC 296-800-28027. https://app.leg.wa.gov/wac/default.aspx?cite=296-800-28027.

"What, How and Why – the Secrets of Schlieren ... - YouTube." Accessed November 15, 2021. https://www.youtube.com/watch?v=3-KnjJ4S7Jo.

White, Frank M. 2016. *Fluid Mechanics.* New York: McGraw-Hill.

Yaw, Louie, and Ralph Stirling. 2016. *Engineering Department Professionalism: Graphing Standards.* Guides and Standards, Walla Walla University.

"You Aren't Gonna Need It." Wikipedia. Wikimedia Foundation, February 1, 2022. https://en.wikipedia.org/wiki/You_aren%27t_gonna_need_it.

Zimmer, Karl. 2021. "Supersonic Flow Nozzle Assembly." Senior Project Paper, Walla Walla University.

XVIII. Appendix A – Device Stand Assembly and Construction Visual Aids

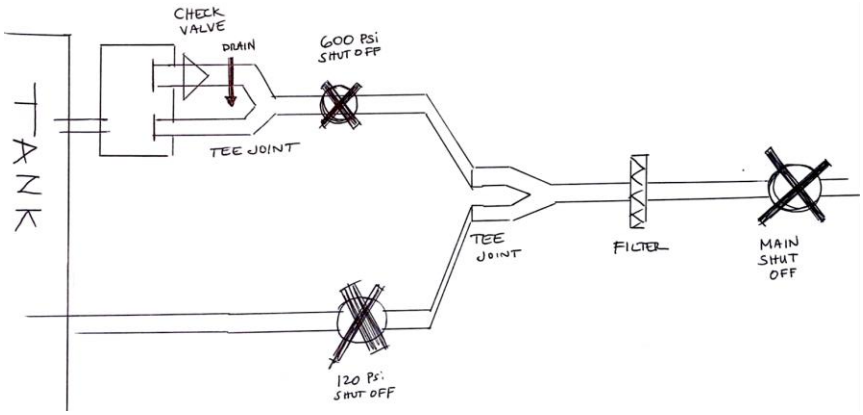

Plumbing Diagram Proposal
Used to convey elements necessary for plumbing upstream of booster pump and 30-gallon tank.

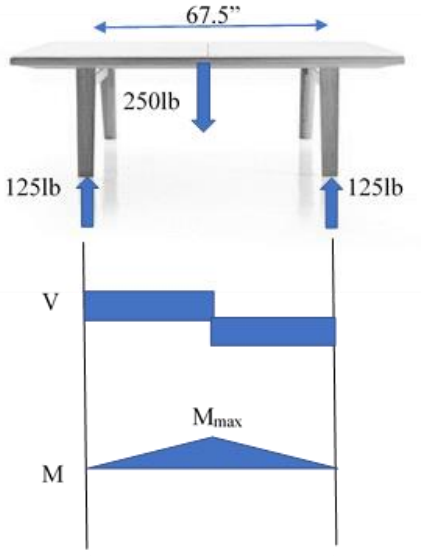

Force Calculation FBD
Free Body models used to convey assumptions made during hand calculations for the design of the device stand.

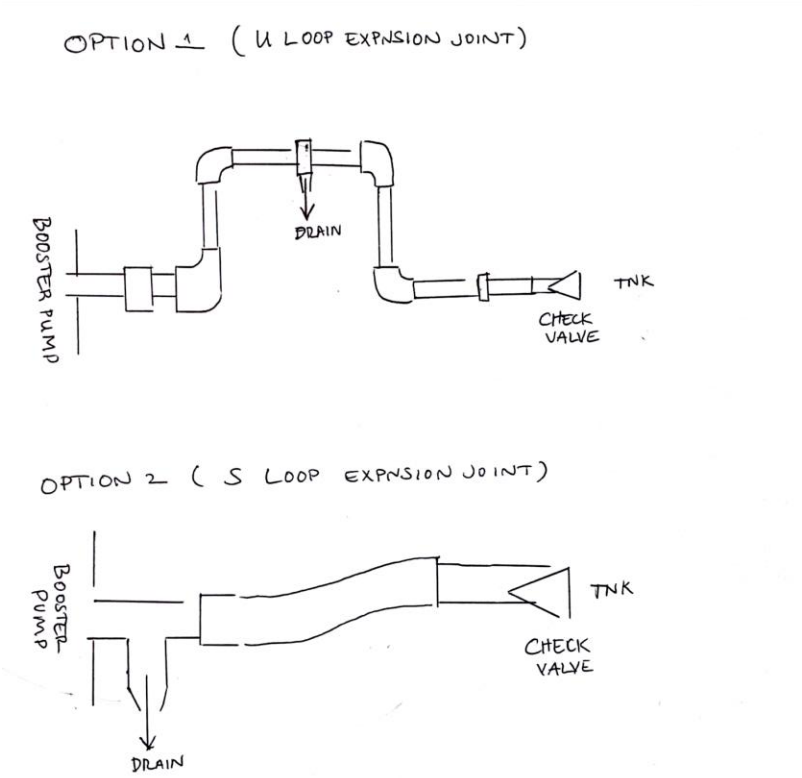

Proposed Downstream Plumbing Diagrams
Diagrams used to convey elements necessary for plumbing downstream of booster pump and 30-gallon tank, considering effects of thermal expansion.

Downstream Plumbing Assembly
Assembly of downstream plumbing from left to right: High pressure Swagelok tee, ball valve drain, high pressure flex hose, high pressure check valve, high pressure valve reducer.

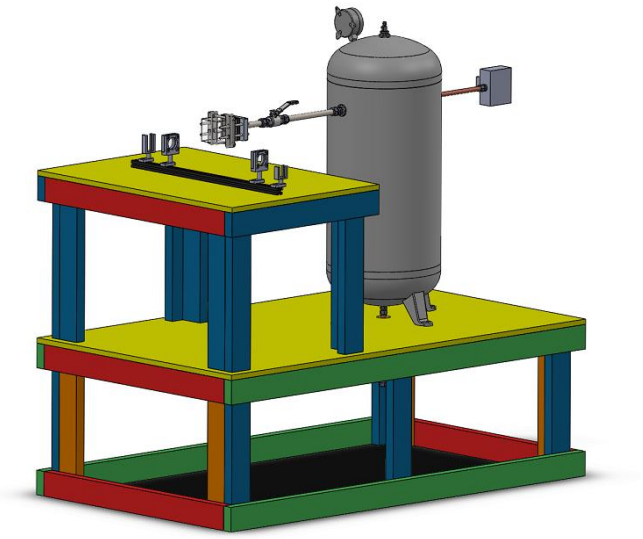

Proposed Device CAD Design
Full assembly model of device created using SOLIDWORKS. This assembly includes the device stand, 30-gallon tank, optics stand, and optics instrumentation.

XIX. Appendix B: Python Code for Calculating Supersonic Flow Properties

The following code makes use of the Python software package written in the course of this project to calculate properties in the nozzle at a variety of different locations and tank pressures.

```
import numpy as np
import units
import supersonic_flow as sf

# Preprocessing
k = 1.4
P_tank_imperial = 600
T_tank_imperial = 68
P_tank = units.psi_to_Pa(P_tank_imperial)
T_tank = units.F_to_K(T_tank_imperial)
R_air = 287.06
rho_tank = P_tank/(R_air*T_tank)
D_crit_imperial = 0.28
D_exit_imperial = 0.57
D_crit = units.in_to_m(D_crit_imperial)
A_crit = np.pi/4*D_crit**2
D_exit = units.in_to_m(D_exit_imperial)
A_exit = np.pi/4*D_exit**2
P_exit_imperial = 14.7
P_exit = units.psi_to_Pa(P_exit_imperial)

nozzle = sf.Nozzle(A_crit, A_exit, T_tank, P_exit, k, R_air)

print("\n\n########################################################")
print("######## Supersonic Nozzle Equations Solver ########")
print("########################################################")
# Solution
radii = np.array([0.3, 0.14, 0.18, 0.22, 0.26])
areas = np.pi*units.in_to_m(radii)**2
pressures_imperial = np.array([600, 550, 500, 450, 400, 350, 300, 250, 200, 150,
100, 50, 40, 30, 20, 14.7])
pressures = units.psi_to_Pa(pressures_imperial)
locations_imperial = np.array([2.756, 3.148, 3.325, 3.547, 3.759])
locations = units.in_to_m(locations_imperial)
data = sf.Dataset(areas, locations, pressures, A_crit, A_exit, T_tank, P_exit, k,
R_air)

data.record()
```

XX. Appendix C: Data Acquisition System Components

Labjack UE9 – Pro

Description:
Analog-to-digital converter (ADC)

Druck UNIK 5000

Description:
Pressure sensor

Dataforth SCM5B38-07

Description:
Strain gage signal conditioner for the pressure sensors

Dataforth SCM5B47-08

Description:
Linearized type-E thermocouple signal conditioner

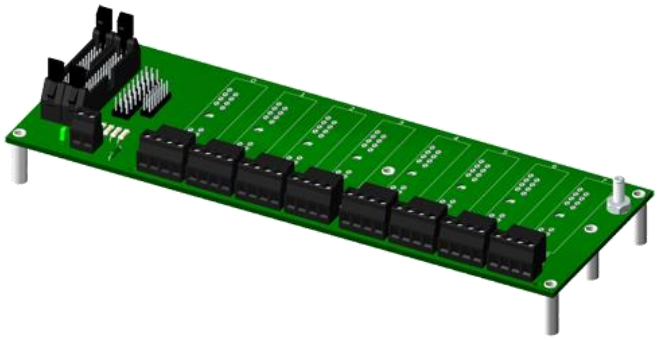

Dataforth SCMPB05

Description:
Non-multiplexed 8 channel back panel with cold-junction compensation

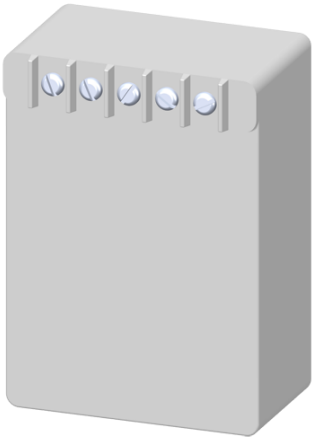

Dataforth SCMXPRT-001

Description:
5 DC volt power supply

Type-E Thermocouple Probe

Description:
Temperature Sensor

Handmade Mount

Description:
A mount for the electronics. The red, 3D-printed piece is meant to hold the pressure sensors. The plexiglass shield on the right is connected to the board by a hinge, and can swing down to cover the electronics.

XXI. Appendix D: Supersonic Nozzle Experiment Laboratory Handout

The phenomenon of compressible flow has been of interest to scientists for a long time, and is an important part of the study of fluid mechanics. Though useful in a variety of contexts such as plasma physics and the medical field, aerospace is where compressible flow is most commonly encountered. When designing aircraft to fly at supersonic speeds, compressible flow develops around the aircraft's wings and body, and must be heavily considered to calculate drag. Additionally, all effective rocket nozzles use a converging-diverging area profile to induce compressible flow, allowing them to produce massive amounts of thrust. In this experiment, you will get to study the characteristics of flow through a converging-diverging nozzle in great detail.

Compressible flow is best understood in the presence of shockwaves. Frank White, an engineering professor at the University of Rhode Island, states that shockwaves are "nearly discontinuous property changes in a supersonic flow" (Fluid Mechanics 10th Edition by Frank White, p. 593). Converging-diverging nozzles create these property changes when air at a certain pressure is released through the nozzle at supersonic speeds. Shockwaves are formed when air is traveling faster than the speed of sound, because when the air inevitably slows down to below the speed of sound, the waves bunch together and form large, discontinuous shifts in the properties of interest. You will get to study some of the characteristics of these shockwaves in this experiment.

Laboratory Description

This laboratory experiment will be conducted using the supersonic nozzle apparatus in the Fluid Mechanics Laboratory. This device uses a booster pump attached to the wall to fill the tank up to 600 psi. This is done through opening the two valves on the wall behind the tank. The nozzle, located on the other side of the tank, can be opened using the valve on that side to run the experiment. The tubes and wires protruding from both the nozzle and the tank are used to measure pressure in the nozzle and the tank, as well as temperature in the tank. Additionally, a schlieren imaging system made up of some lenses, a light, and a camera is used to capture the density gradients around the outlet of the nozzle, and this is also recorded in the form of a video. This data is fed to the computer, which you will be using to obtain the data from the experiment.

Additionally, the experiment has a valve that emerges beneath the table the tank is sitting on. This is used to drain out any condenses water that builds up in the tank during the experiment.

Theory

There are several properties of the fluid that are important to consider when studying compressible flow in converging-diverging nozzles:

$$\text{Ma} = \text{non-dimensional velocity} = \frac{V}{a}$$

$$a = \text{speed of sound} = \sqrt{kRT}$$
$$V = \text{velocity}, P = \text{pressure}, T = \text{temperature}, \rho = \text{density}$$

Only two are used directly in this laboratory experiment: pressure (P) and Mach number (Ma). In an ideal converging-diverging nozzle, under the assumption that all compressible flow being studied is isentropic and adiabatic, the area relation below makes it possible to find the Mach number at any point in the nozzle:

$$\frac{A}{A^*} = \frac{1}{M_a}\left[\left(\frac{2}{k+1}\right)\left(1 + \frac{k-1}{2}M_a^2\right)\right]^{(k+1)/[2(k-1)]} \quad (1)$$

Note that with this relation, there will always be two Mach numbers possible for a given location: a supersonic one, and a subsonic one. If this equation is too daunting to solve, the **Isentropic Compressible Flow Table**, attached to this handout, can be interpolated in place of the equation.

Once Mach number is known, the isentropic relation given below can be used to find the pressure at any point in the nozzle:

$$\frac{P_0}{P} = \left(1 + \frac{k-1}{2}M_a^2\right)^{k/(k-1)} \quad (2)$$
$$P_0 = \text{stagnation pressure} = \text{tank pressure}$$

Normal Shockwaves

When a normal shockwave is present in the nozzle, the normal shock relations given below must be used find Mach number, pressure, and an altered critical area on one side given the properties on the other:

$$Ma_2^2 = \frac{(k-1)Ma_1^2 + 2}{2kMa_1^2 + 2} \quad (3a)$$

$$\frac{P_2}{P_1} = \frac{1}{k+1}[2kMa_1^2 - (k-1)] \quad (3b)$$

$$\frac{A_2^*}{A_1^*} = \left[\frac{2 + (k-1)Ma_1^2}{2 + (k-1)Ma_2^2}\right] \quad (3c)$$

Note here that the upstream properties are labeled with a 1, and the downstream properties are labeled with a 2. If equation $(3a)$ is difficult to solve, the **Normal Shock Mach Number Table**, attached to this handout, can be interpolated in place of the equation, similar to equation (1).

Oblique Shockwaves

Finally, in the case of an oblique shockwave, the normal shockwave equations still apply, with one modification. An oblique shockwave is a shockwave that fans out from the nozzle, as shown:

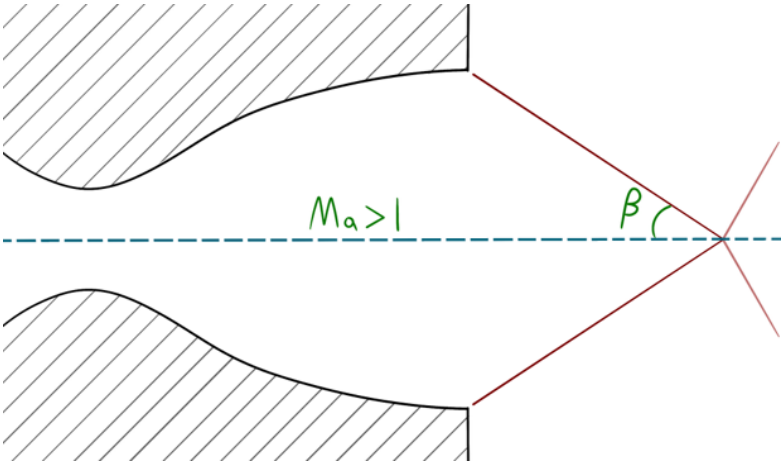

Dealing with such a case is actually quite simple. Since the Mach number is actually approaching the shockwave at an angle, we simply need to take its normal component to the shockwave:

$$\mathrm{Ma_n} = \mathrm{Ma}\sin\beta = \text{Mach number normal to the shockwave} \quad (4)$$
$$\beta = \text{Oblique shockwave angle, as shown in the image}$$

Now, equations $(3a)$, $(3a)$, and $(3a)$ can be used. Simply find the normal Mach number, use the normal shock equations, and, if needed, convert the Mach number on the other side to the actual Mach number again.

Maximum Thrust

Converging-diverging nozzles are often used in aerospace to produce thrust. The thrust of such a nozzle is maximized when the oblique shockwaves are parallel, at which point the thrust is given by the following equation:

$$F_{max} = kP_eA_e\mathrm{Ma}_e^2 \quad (5)$$

For more information about these equations, how they are used, and how they were derived, review sections 9.3-9.5 (p. 600-618) and 9.9 (p. 642-650) *Fluid Mechanics 10th Edition* by Frank White.

Experimental Procedure

In order to run the experiment and collect meaningful data from it for your laboratory report, you must follow a number of steps:

1. Preparation (Possible will be done when you arrive)
    A. Measure the atmospheric pressure in the laboratory using the barometer located on the wall. Make sure to record this in your report as P_{atm}.
    B. Record this value on the computer where indicated by the software and click the "Recalibrate" button.
    C. Open the three valves before the booster pump to fill the tank up to around 600 psi.
    D. Close the three valves before the booster pump.
2. Experiment
    A. Find the proper page in the software and click the start button.

B. Once you are sure the computer is recording, open the valve.
C. Allow the experiment to run, and observe the behavior of the shockwaves on the computer screen.
D. Once it appears the tank has reached atmospheric pressure and the nozzle is no longer blowing, stop the recording and save your session.

3. Data Recording
   A. Using the software, replay the session. Pause the session at the spots where the shockwaves are parallel, at 45 degrees, and the moment when the shockwaves go from being oblique to normal. At each of these three data points, record tank pressure.
   B. Locate the excel file that contains all the data from the experiment. It will have been saved in a folder somewhere by the software.
   C. Note that the data refers to several different pressures. P0 is the pressure in the tank. P1, P2, P3, and P4 are pressures as measured through four taps in the nozzle, as shown in the following image. Cross-sectional areas at each location are also recorded below, for use in compressible flow calculations.

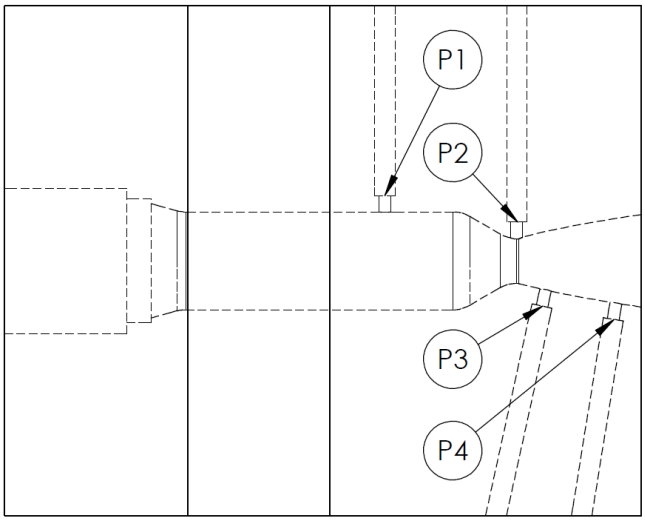

Tap	Area (in²)
P1	0.283
P2	0.062
P3	0.102
P4	0.202

Required Calculations

The laboratory report will require four types of calculations to be done in order to categorize the data. These calculations are outlined below, referring to equations in the **Theory** section.

P_0 and thrust when oblique shockwaves are parallel ($P_{0,max\ thrust}$, F_{max})

This is also the pressure in the tank when the nozzle is at maximum thrust.

Known:

Pressure at the exit is the same as the atmosphere ($P_e = P_{atm}$)
Pressure at the exit is supersonic

Unknown:

Pressure in the tank ($P_{0,\max\text{ thrust}}$)

Maximum thrust of the nozzle ($F_{\max}$)

Solution:

1. Find Mach number at the exit using equation (1)
2. Find $P_{0,\max\text{ thrust}}$ using equation (2)
3. Find $F_{\max}$ using equation (5)

P_0 when there is a normal shockwave at the exit ($P_{0,min\ super}$)

When P_0 is lower than this value, then there is either a shockwave inside the nozzle, or no shockwave at all.

Known:

Pressure at the exit is the same as the atmosphere ($P_e = P_{atm}$)

A shockwave exists at the exit

Unknown:

Pressure in the tank ($P_{0,\min\text{ super}}$)

Solution:

1. Find the supersonic Mach number before the shockwave using equation (1)
2. Find the Mach number after the shockwave using equation $(3a)$
3. Find the pressure before the shockwave using equation $(3b)$
4. Find $P_{0,\min\text{ super}}$ using equation (2)

P_0 when there is just barely a shockwave at the throat ($P_{0,max\ sub}$)

When P_0 is lower than this value, then there is no shockwave at all. If it is higher, a shockwave must exist somewhere.

Known:

Pressure at the exit is the same as the atmosphere ($P_e = P_{atm}$)

Mach number is exactly 1 at the throat

Mach number at the exit is subsonic

Unknown:

Pressure in the tank ($P_{0,\max\text{ sub}}$)

Solution:

1. Find the subsonic Mach number at the exit using equation (1)
2. Find $P_{0,\max\text{ sub}}$ using equation (2)

P_0 when there a shockwave at either pressure measurement point after the throat

This is actually two identical calculations, except the area changes for each.

Known:

Pressure at the exit is the same as the atmosphere ($P_e = P_{atm}$)
There is a shockwave where the measurement takes place (A)
Mach number at the exit is subsonic

Unknown:

Pressure in the tank (P_0)

Solution:

1. Find the supersonic Mach number before the shockwave using equation (1)
2. Find the Mach number after the shockwave using equation $(3a)$
3. Find the adjusted critical area after the shockwave using equation $(3c)$
4. Find the subsonic Mach number at the exit using equation (1) and the new critical area
5. Find the pressure right after the shockwave using equation (2)
6. Find the pressure right before the shockwave using equation $(3b)$
7. Find P_0 using equation (2) and the original critical area

Required Graphs

The laboratory report will require three separate graphs. They are listed and described below.

P/P_0 vs A/A^*

1. Plot the theoretical curve for this graph using equations (1) and (2) from the **Theory** section of this handout. You can accomplish this by choosing an even spread of Mach numbers over which to calculate the two values, and then using those to generate both values.
2. Plot the actual data gathered from the experiment on the same graph. Split the data into four groups, distinguished by either color, shape, or both. These groups are defined by the pressure in the tank as follows:
    a. Oblique shockwave angle exceeds parallel

$P_0 > P_{0,\max\ thrust}$

    b. Oblique shockwave angle is less than parallel

$P_{0,\max\ \text{thrust}} > P_0 > P_{0,\min\ \text{super}}$

    c. A shockwave is present inside the nozzle

$P_{0,\min\ \text{super}} > P_0 > P_{0,\max\ \text{sub}}$

    d. No shockwave is present

$P_{0,\max\ \text{sub}} > P_0$

β vs P_0/P_{atm}

1. Plot the theoretical curve for this graph for a range of equally spaced tank pressures in the region where oblique shockwaves are present, but less than parallel

$$P_{0,max\ \text{thrust}} > P_0 > P_{0,\min\ \text{super}}$$

For each P_0:

   a. Use equation (1) to find the Mach number at the exit of the nozzle
   b. Use equation (2) to find the pressure at the exit of the nozzle
   c. Use equation (4) alongside equation $(3a)$ to find β
2. Plot the three data points gathered from the experiment for the three angles of β on the same graph.

P/P_0 vs P_0/P_{atm}

Produce this graph, as described below, for all measured points. This will produce a total of four graphs, three with vertical lines in addition to the data and one with only the data.

1. Plot a vertical line at the tank pressure where you calculated the shockwave should be present at *this point* in the nozzle, if this point is the throat or one of the two points downstream of it.
2. Plot the actual data gathered from the experiment *for this point only* on the same graph.

Required Questions

In your laboratory report, you will need to address the following questions. They are arranged in categories based on the calculations they are related to.

P/P_0 vs A/A^*

A. How does the actual data compare with the theoretical curve?
B. Do the categories match cleanly with the changes in behavior you observe on the graph? If not, how do they differ, and what does that suggest?
C. Are there any regions of data that seem to have a large discrepancy with this curve? If so, why?

β vs P_0/P_{atm}

A. How does the actual data you took compare with the theoretical curve?
B. Do the two datapoints at $\beta = 90°$ and $\beta = 0°$ match with the calculated values $P_{0,max\ thrust}$ and $P_{0,\min \text{ super}}$? If not, why do you think that is?

P/P_0 vs P_0/P_{atm}

A. Describe the behavior of the pressure at each of the four plots over time as the tank pressure decreased. Does the behavior match what you would expect for a converging-diverging nozzle?
B. Does the vertical line correspond to the behavior of the pressures for each of the three graphs where shockwaves are possible? If so, explain how and why that is. If not, discuss why it does not.

Thrust

A. Does the order of magnitude of thrust you calculated make sense to you? How would it compare to the actual thrust of a jet engine? If similar, why would it be similar? If different, why would it be different?

Additional Questions

A. It is probable that some of your data did not line up with the theoretical results you expected. What factors do you think lead to non-ideal results? And do you see that effect in your data? What sources of error might be responsible for each difference noted?
B. Are there any other sources of error in this experiment that you can think of? How might they impact the data?

Isentropic, Compressible Flow Table

***Fluid Mechanics 10th Edition* by Frank White, p. 813**

Ma	P/P_0	A/A*	Ma	P/P_0	A/A*
0.00	1.0000	∞	2.10	0.1094	1.8369
0.10	0.9930	5.8218	2.20	0.0935	2.0050
0.20	0.9725	2.9635	2.30	0.0800	2.1931
0.30	0.9395	2.0351	2.40	0.0684	2.4031
0.40	0.8956	1.5901	2.50	0.0585	2.6367
0.50	0.8430	1.3398	2.60	0.0501	2.8960
0.60	0.7840	1.1882	2.70	0.0430	3.1830
0.70	0.7209	1.0944	2.80	0.0368	3.5001
0.80	0.6560	1.0382	2.90	0.0317	3.8498
0.90	0.5913	1.0089	3.00	0.0272	4.2346
1.00	0.5283	1.0000	3.10	0.0234	4.6573
1.10	0.4684	1.0079	3.20	0.0202	5.1210
1.20	0.4124	1.0304	3.30	0.0175	5.6286
1.30	0.3609	1.0663	3.40	0.0151	6.1837
1.40	0.3142	1.1149	3.50	0.0131	6.7896
1.50	0.2724	1.1762	3.60	0.0114	7.4501
1.60	0.2353	1.2502	3.70	0.0099	8.1691
1.70	0.2026	1.3376	3.80	0.0086	8.9506
1.80	0.1740	1.4390	3.90	0.0075	9.7990
1.90	0.1492	1.5553	4.00	0.0066	10.7188
2.00	0.1278	1.6875			

Normal Shock Mach Number Table

***Fluid Mechanics 10th Edition* by Frank White, p. 814**

Ma_1	Ma_2	Ma_1	Ma_2
1.00	1.0000	3.10	0.2205
1.10	0.9118	3.20	0.4643
1.20	0.8422	3.30	0.4596
1.30	0.7860	3.40	0.4552
1.40	0.7397	3.50	0.4512
1.50	0.7011	3.60	0.4474
1.60	0.6684	3.70	0.4439
1.70	0.6405	3.80	0.4407
1.80	0.6165	3.90	0.4377
1.90	0.5956	4.00	0.4350
2.00	0.5774	4.10	0.4324
2.10	0.5613	4.20	0.4299
2.20	0.5471	4.30	0.4277
2.30	0.5344	4.40	0.4255
2.40	0.5231	4.50	0.4236
2.50	0.5130	4.60	0.4217
2.60	0.5039	4.70	0.4199
2.70	0.4956	4.80	0.4183
2.80	0.4882	4.90	0.4167
2.90	0.4814	5.00	0.4152
3.00	0.4752		